[19] Tozawa H, Andoh S, Takayama Y, Tanaka Y, Lee B, Nakamura H, et al. Species-dependent antigenicity of the 34-kDa glycoprotein found on the membrane of various primate lymphocytes transformed by human T-cell leukemia virus type-I (HTLV-I) and simian T-cell leukemia virus (STLV-I). Int J Cancer 1988;41: 231-8.
[20] Takahashi Y, Tanaka Y, Yamashita A, Koyanagi Y, Nakamura M, Yamamoto N. OX40 stimulation by gp34/OX40 ligand enhances productive human immunodeficiency virus type 1 infection. J Virol 2001;75:6748-57.
[21] Baba E, Takahashi Y, Lichtenfeld J, Tanaka R, Yoshida A, Sugamura K, et al. Functional CD4 T cells after intercellular molecular transfer of OX40 ligand. J Immunol 2001;167:875-83.
[22] Traggiai E, Chicha L, Mazzucchelli L, Bronz L, Piffaretti JC, Lanzavecchia A, et al. Development of a human adaptive immune system in cord blood cell-transplanted mice. Science 2004;304:104-7.
[23] Rizza P, Santini SM, Logozzi MA, Lapenta C, Sestili P, Gheradi G, et al. T-cell dysfunctions in hu-PBL-SCID mice infected with human immunodeficiency virus (HIV) shortly after reconstitution: in vivo effects of HIV on highly activated human immune cells. J Virol 1996;70:7958-64.
[24] Rogers PR, Dong J, Gramalia I, Killeen N, Croft M. OX40 promotes Bcl-xL and Bcl-2 expression and is essential for long-term survival of CD4 T cells. Immunity 2001;15:445-55.
[25] Yoshida H, Kawane K, Koike M, Mori Y, Ushiyama Y, Nagata S. Phosphatidylserine-dependent englfment by macrophages of nuclei from erythroid precursor cells. Nature 2005;437:754-8.
[26] Zhang LF, Okuma K, Tanaka R, Kodama A, Kondo K, Ansari AA, et al. Generation of mature dendritic cells with unique phenotype and function by in vitro short-term culture of human monocytes in the presence of interleukin-4 and interferon-beta. Exp Biol Med 2008;233:721-31.
[27] Johansson U, Walther JL, Smed SA, Spetz AL. Triggering of dendritic cell responses after exposure to activated, but not resting, apoptotic PBMCs. J Immunol 2007;179:1711-20.
[28] Morris NP, Peters C, Montler R, Hu HM, Curti BD, Urba WJ, et al. Development and characterization of recombinant human Fc: OX40L fusion protein linked via a coiled-coil trimerization domain. Mol Immunol 2007;44:3112-21.
[29] Muller N, Wyzgol A, Munkel S, Pfizenmaier K, Wajant H. Activity of soluble OX40 ligand is enhanced by oligomerization and cell surface immobilization. FEBS J 2008;275:2296-304.
[30] Ruby CE, Redmond WL, Haley D, Weinberg AD. Anti-OX40 stimulation in vivo enhances CD8+ memory T cell survival and significantly increases recall responses. Eur J Immunol 2007;37: 157-66.
[31] Ndhlovu LC, Takeda I, Sugamura K, Ishii N. Expanding role of T-cell costimulators in regulatory T-cell function: recent advances in accessory molecules expressed on both regulatory and nonregulatory T cells. Crit Rev Immunol 2004;24:251-66.
[32] Redmond WL, Weinberg AD. Targeting OX40 and OX40L for the treatment of autoimmunity and cancer. Crit Rev Immunol 2007;27:415-36.
[33] Salek-Ardakani S, Croft M. Regulation of CD4 T cell memory by OX40 (CD134). Vaccine 2006;24:872-83.
[34] Song A, Tang X, Harms KM, Croft M. OX40 and Bcl-xL promote the persistence of CD8 T cells to recall tumor-associated antigen. J Immunol 2005;175:3534-41.
[35] Piconese S, Valzasina B, Colombo MP. OX40 triggering blocks suppression by regulatory T cells and facilitates tumor rejection. J Exp Med 2008;205:825-39.
[36] Colombo MP, Piconese S. Regulatory-T-cell inhibition versus depletion: the right choice in cancer immunotherapy. Nat Rev Cancer 2007;7:880-7.
[37] Tanaka H, Demeure CE, Rubio M, Delespesse G, Sarfati M. Human monocyte-derived dendritic cells induce naive T cell differentiation into T helper cell type 2 (Th2) or Th1/Th2 effectors. Role of stimulator/responder ratio. J Exp Med 2000;192: 405-12.
[38] Morimoto S, Kanno Y, Tanaka Y, Hashimoto H, Jacquot S, Morimoto C, et al. CD134L engagement enhances human B cell Ig production: CD154/CD40, CD70/CD27, and CD134/CD134L interactions coordinately regulate T cell-dependent B cell responses. J Immunol 2000;164:4097-104.
[39] Fujita T, Kambe N, Uchiyama T, Hori T. Type I interferons attenuate T cell activating functions of human mast cells by decreasing TNF-alpha production and OX40 ligand expression while increasing IL-10 production. J Clin Immunol 2006;26: 512-8.
[40] Murata S, Ladle BH, Kim PS, Lutz ER, Wolpoe ME, Ivie SE, et al. OX40 costimulation synergizes with GM-CSF whole-cell vaccination to overcome established CD8+ T cell tolerance to an endogenous tumor antigen. J Immunol 2006;176:974-83.
[41] Higashimura N, Takasawa N, Tanaka Y, Nakamura M, Sugamura K. Induction of OX40, a receptor of gp34, on T cells by trans-acting transcriptional activator, Tax, of human T-cell leukemia virus type 1. Jpn J Cancer Res 1996;87:227-31.
[42] Wang Q, Chen Y, Xie F, Ge Y, Chen L, Wu H, et al. Development of a sandwich ELISA for evaluating soluble OX40L (CD252) in human sera of different ages or with Graves' disease. Cytokine 2006;36:23-8.
[43] Kim KM, Kim HW, Kim JO, Beak KM, Kim JK, Kang CY. Induction of 4-1BB (CD137) expression by DNA damaging agents in human T lymphocytes. Immunology 2002;107:472-9.
[44] Ma BY, Mikolajczak SA, Danesh A, Hosiawa KA, Cameron CM, Takaori-Kondo A, et al. The expression and the regulatory role of OX40 and 4-1BB heterodimer in activated human T cells. Blood 2005;106:2002-10.

Generation of Mature Dendritic Cells with Unique Phenotype and Function by *In Vitro* Short-Term Culture of Human Monocytes in the Presence of Interleukin-4 and Interferon-β

LI FENG ZHANG,* KAZU OKUMA,* REIKO TANAKA,* AKIRA KODAMA,* KAYO KONDO,* AFTAB A. ANSARI,† AND YUETSU TANAKA*,[1]

Department of Immunology, Graduate School of Medicine, University of the Ryukyus, Nishihara-cho, Okinawa, Japan; and †Department of Pathology, Emory University School of Medicine, Atlanta, Georgia 30322

Dendritic cell (DC)-based immunotherapy has been utilized for the treatment of not only a number of human malignancies but also a select group of infectious diseases. Conventional techniques for the generation and maturation of DCs require 7 days of *in vitro* culture, which prompted us to seek alternative methods that would hasten the generation of functional human myeloid DCs *in vitro*. Following the use of a number of cytokines/growth factors, we found that *in vitro* culture of purified human monocytes, in media containing interleukin (IL)-4, together with interferon (IFN)-β for 24 hrs, followed by the addition of non-specific antigenic stimuli, such as keyhole limpet hemocyanin (KLH), lipopolysaccharide (LPS), or inactivated human immunodeficiency virus (HIV)-1 induced the monocytes to differentiated by 3 days into mature DCs (4B-DCs). These 4B-DCs expressed high levels of CD83 and CD11c, as well as markers of immune activation, including CD80 and CD86, human leukocyte antigen (HLA) class I and II, and CD14, but not CD1a. Anti-CD14 blocking antibody interfered with generation of 4B-DCs by LPS, but not by KLH or HIV-1. Interestingly, 4B-DCs, but not conventional DCs generated using macrophage-colony stimulating factor and IL-4 (G4-DCs), expressed OX40 and OX40L. 4B-DCs showed phagocytic activity, and spontaneously produced IL-12 and tumor necrosis factor (TNF)-α, but not IL-10. 4B-DCs promoted proliferation of allogeneic naïve $CD4^+$ T cells, producing IFN-γ at lower levels than those stimulated with G4-DCs. 4B-DCs were more potent stimulators of allogeneic bulk $CD8^+$ T cells producing IFN-γ than G4-DCs. These data indicate that 4B-DCs are unique and may provide a relatively more rapid alternative tool for potential clinical use, as compared with conventional G4-DCs. Exp Biol Med 233:721–731, 2008

Key words: dendritic cell, IL-4, type-I IFN, immune stimulation, OX40, human monocytes

Introduction

Dendritic cells (DCs) are professional antigen-presenting cells that play crucial roles in the initiation and regulation of immune responses (1). DCs reside in an immature state at the sites of potential pathogen entry, and generally recognize invading pathogens via a family of Toll-like receptors (TLRs), complement receptors, and lectin receptors (2). This interaction with pathogens induces DCs to undergo maturation and migrate into secondary lymphoid organs, where they present processed forms of the antigen to stimulate antigen-specific T cells, and thus initiate immune responses (3). Results from a number of recent studies have highlighted the potential of DCs to serve as natural cellular "adjuvants" (4). This functional attribute has led to clinical trials of DC-based immunotherapy for not only a number of animal tumor models and human malignancies (5) but also against a number of infectious disease agents. This view is highlighted by the recent finding that immunization of human immunodeficiency virus type 1 (HIV-1) infected patients with autologous DCs sensitized with chemically inactivated autologous HIV-1 led to a marked sustained decrease in viral load (6, 7), which was reasoned to be

This work was supported in part by grants from a Grant-in-Aid for Research on HIV/AIDS and Health Sciences focusing on Drug Innovation from the Ministry of Health, Labor and Welfare of Japan; and Japan Human Science Foundation.

[1] To whom correspondence should be addressed at Department of Immunology, Graduate School of Medicine, University of the Ryukyus, Uehara 207, Nishihara-cho, Nakagami-gun, Okinawa 903-0215, Japan. E-mail: yuetsu@s4.dion.ne.jp

Received December 12, 2007.
Accepted January 4, 2008.

DOI: 10.3181/0712-RM-333
1535-3702/08/2336-0721$15.00

secondary to DC-mediated enhancement of both virus-specific cellular and neutralizing antibody-responses. This finding was further supported utilizing a human peripheral blood leukocyte-populated severe combined immune deficiency (hu-PBL-SCID) mouse model, in which the human peripheral blood mononuclear cell (PBMC)-engrafted mice, following immunization with inactivated HIV-1-pulsed conventional DCs, were shown to generate higher relative levels of HIV-1-specific T- and B-cell immune responses sufficient to protect these animals against challenge with virulent HIV-1 isolates (8, 9).

A variety of methodologies to generate functional DCs *in vitro* have been published. The findings from these studies show that the phenotype and function of *in vitro* monocyte-derived DCs are influenced by a wide variety of factors, including methods utilized to isolate and prepare purified populations of monocytes and the *in vitro* culture conditions utilized (10). Immunostimulating myeloid DCs have been conventionally generated *in vitro* by culturing human peripheral blood monocytes in the presence of granulocyte and granulocyte macrophage colony-stimulating factor (GM-CSF) together with interleukin (IL)-4 for 4–6 days followed by maturation stimuli for 1–2 days. In order to acquire functional immunostimulating capacity, DCs need to mature because immature DCs have been shown to be immunosuppressive due to their ability to selectively induce the generation and expansion of regulatory T cells (Treg) (11). Thus, conventional immature DCs have been used following maturation by incubation in media containing tumor necrosis factor (TNF)-α, CD40 ligand, or lipopolysaccharide (LPS). Type-I interferon (IFN-α and IFN-β) has also been used to mature immature DCs (12, 13). Recently, attempts have been made to reduce the time required for preparing mature DCs *in vitro* aimed at reducing the cost and the labor involved. One representative method is to incubate the enriched population of monocytes in a cocktail of IL-6, IL-1β, TNF-α and prostaglandin E_2 (PGE_2) on day 1 following the culture of monocytes in GM-CSF and IL-4 (14, 15). Another method described proposes the use type-I IFN and GM-CSF (12, 16). Although several lines of evidence exist that suggest the inhibitory nature of type-I IFN for the generation of myeloid DCs *in vitro* (17, 18), results from other studies show that type-I IFN-derived myeloid DCs are potent stimulators for antigen-specific not only $CD4^+$ T, but also $CD8^+$ T cell responses including those against HIV-1 (13, 16, 19, 20).

The use of type-I IFN by some and IL-4 by others for the *in vitro* maturation of DCs (21, 22) prompted our laboratory to test whether the use of these two cytokines in combination in the absence of GM-CSF could facilitate differentiation of functional DCs during a short-term culture period. We herein report the results of our findings that document our success in the generation of functional DCs from monocytes within 3 days that are distinct from conventional DCs in phenotype, cytokine production, and function.

Materials and Methods

Reagents. Medium used throughout these studies consisted of RPMI-1640 supplemented with 5% heat-inactivated fetal calf serum (FCS; Sigma, St. Louis, MO), 100 U/ml penicillin, and 100 μg/ml streptomycin (hereafter referred to as RPMI medium). The recombinant human cytokines used included human IL-4, GM-CSF (PeproTech, London, UK), IFN-β (Torey, Tokyo, Japan), and IL-2 (provided by the National Institutes of Health Acquired Immune Deficiency Syndrome [AIDS] Research and Reference Reagent Program). Anti-human CD3 (OKT-3) and anti-human CD28 monoclonal antibodies (mAb) were obtained from ATCC (Manassas, VA) and R&D Systems, Inc. (Minneapolis, MN), respectively. Aldrithiol-2 (AT-2), keyhole limpet hemocyanin (KLH), LPS from *Escherichia coli,* and low-endotoxin bovine serum albumin (BSA) were purchased from Sigma Chemical. A human monocyte negative isolation and a human naïve $CD4^+$ T cell isolation kit were purchased from Dynal Biotec Inc. (Oslo, Norway) and Miltenyi Biotec (Gladbach, Germany), respectively. Enzyme-linked immunosorbent assay (ELISA) kits for human IL-12 p70 and TNF-α were purchased from Biosource International, Inc. (Camarillo, CA). ELISA kits for human IL-10 and IFN-γ were purchased from R&D Systems, Inc. A bromodeoxyuridine (BrdU)-incorporated ELISA kit was purchased from Roche Diagnostics (Mannheim, Germany). The Vybrant carboxyfluorescein succinimidyl ester (CFSE) cell tracer kit and fluorescein isothiocyanate (FITC)-labeled *E. coli* (FITC-*E. coli*) were purchased from Invitrogen (Carlsbad, CA). Fluorescent-dye labeled mouse mAbs used included FITC-IgG1 anti-CD80, FITC-IgG2a anti-CD1a, FITC-IgG2b anti-human leukocyte antigen (HLA)-DR, phycoerythrin (PE)-IgG1 anti-CD11c, PE-IgG2b anti-CD86, Cy5-IgG2a anti-CD14, Cy5-IgG1 anti-CD3, FITC- or PC5-IgG2b anti-CD83, PE-IgG2a anti-CCR7 (BD Pharmingen, San Diego, CA), PE-IgG2a anti-HLA-ABC (DAKO, Glostrup, Denmark), and isotype-matched control mAbs (Beckman Coulter, Fullerton CA). Anti-human CCR5 used was Cy5-IgG1 (rat) anti-human CCR5 (clone T312) (23). For examination of OX40 and its ligand (OX40L), fluorescently labeled or unlabeled mouse IgG1 anti-human OX40 (clone B7B5) (24), anti-human OX40L (clone TAG34) (25), or control IgG1 (clone TAXY7) (26) were used in combination with FITC-goat anti-mouse IgG (American Qualex, San Clemente, CA). A rat IgG1 anti-OX40 mAb, W4–54, was used to block intercellular transfer of OX40 (27).

Generation of DCs. PBMCs were isolated from heparinized peripheral blood obtained from normal healthy adult volunteer donors by a density gradient centrifugation method on lymphocyte separation medium (Sigma Chemical). Cells at the interface were collected and washed three times in cold phosphate-buffered saline (PBS) containing 0.1% low-endotoxin BSA and 2 m*M* Na_2-EDTA. Monocytes were purified from these PBMCs by using the $CD14^+$

monocyte negative isolation kit. An aliquot of cells from each monocyte preparation was examined by flow cytometry and found to contain >90% $CD14^+$ cells. These monocytes were resuspended at a concentration of 5×10^5 cells/ml in RPMI medium and 0.5~1.0 ml of cell suspension was dispensed into individual wells of 24-well plates (BD Pharmingen), and then cultured in the presence of IL-4 (10 ng/ml) and IFN-β (1000 U/ml) at 37°C in a 5% CO_2 humidified incubator for 3 days. The cultures were pulsed at different time points with either KLH (10 μg/ml), LPS (10 ng/ml), or HIV-1_{IIIB} (p24 level of 10 ng/ml). The HIV was inactivated with Aldrithiol-2 as described previously (9) prior to its addition to the cultures. Cultures containing conventional DCs were prepared in parallel for purposes of comparison designed to mature concurrently with the DCs generated according to our modified protocol. The conventional DCs were derived by culturing the enriched population of monocytes in the presence of GM-CSF (500 ng/ml) and IL-4 (20 ng/ml) for 5 days followed by maturation by the addition of 1000 U/ml IFN-β treatment for an additional 2 days (9).

Flow Cytometry. Aliquots of the cells to be analyzed were incubated in PBS containing 0.1% BSA and 0.1% NaN_3 (fluorescence activated cell sorting [FACS] buffer) supplemented with 2 mg/ml normal human IgG on ice for 15 min to block Fc receptors. The cell suspension was then incubated with a predetermined optimal concentration of the appropriate fluorescently labeled mAbs against human cell surface molecules on ice for 30 min. In some experiments, cells were indirectly stained with mouse mAbs at 2.5 μg/ml for 30 min, followed by goat anti-mouse IgG-FITC. After washing with FACS buffer, cells were fixed in 1% paraformaldehyde (PFA)-containing FACS buffer. The cells were analyzed by standard flow cytometry using a FACS-Calibur assisted by Cell Quest software (BD Pharmingen).

Phagocytic function was examined using FITC-labeled *E. coli* as described previously (28). Briefly, sample cells (2×10^5) in 0.2 ml of RPMI medium were incubated with FITC-*E. coli* particles at a cell to bacterium ratio of 1:15 for 30 min at 37°C in a 5% CO_2 humidified incubator. The mixture was washed twice with FACS buffer, and fixed with FACS buffer containing 1% PFA. The relative levels of uptake of FITC-*E. coli* by the cells were determined by standard flow cytometry.

Stimulation of Naïve $CD4^+$ T and Bulk $CD8^+$ T Cells. Enriched population of naïve $CD4^+$ T cells (2×10^4/ml) were isolated from normal human PBMCs by using the naïve $CD4^+$ T cell isolation kit (>90% purity as assessed by FACS analysis), and then cocultured with allogeneic DCs (0.5×10^4 cells/ml) in RPMI medium without the exogenous addition of IL-2 in 96-well U-bottom plates (BD Pharmingen) in a volume of 0.2 ml/well. Cultures were performed in triplicate. After 7 days, cell proliferation was assessed by using the BrdU-incorporation ELISA kit. CFSE-labeling of T cells was carried out according to the manufacturer's protocol. CFSE-labeled or unlabeled $CD8^+$ T cells were stimulated with allogeneic DCs at a DC to T cell ratio of 1:4 in RPMI medium supplemented with IL-2 (20 U/ml) in 96-well U-bottom plate for 5 days. Proliferation of CFSE-labeled $CD8^+$ T cells was assessed by standard flow cytometry. For expansion of $CD4^+$ T cells stimulated by DCs, the $CD4^+$ T cells were stimulated with immobilized OKT-3 mAb (5 μg/ml) and soluble anti-CD28 mAb (1 μg/ml) in IL-2-free RPMI medium for 3 days.

Treg Assay. CFSE-labeled naïve $CD4^+$ T cells (2×10^4/well) were cocultured with autologous highly enriched population of $CD14^+$ cells (2×10^4/well). The $CD14^+$ cells were precoated with anti-CD3 mAb (OKT-3) that bound the $CD14^+$ cells via the Fc receptors. These cocultures were incubated in the presence or absence of varying numbers of cells being tested for Treg activity. Thus, $CD4^+$ T cells that were cocultured with allogeneic 4B-DC or G4-DC were tested for their ability to serve as Tregs. In addition, $CD4^+$ T cells restimulated with anti-CD3/CD28 mAb (2×10^4 cells/well) were subsequently assessed for Treg activity. Cultures were performed in triplicate using 96-well U-bottom plates. Following coculture with the Tregs for 3 days, the cells were harvested and the CFSE profile of the responder cells was examined by standard flow cytometry.

***In Vitro* HIV-1 Infection Assay.** Sensitivity of DCs to infection *in vitro* with HIV-1 R5 strain JR-CSF was determined as follows. Target DCs were washed and dispended into wells of a 96-well U-bottomed plate at 1×10^5 cells/well in a volume of 0.1 ml of RPMI medium and then infected with R5 HIV-1 JR-CSF at a multiplicity of infection (m.o.i.) of 0.1 and incubated overnight at 37°C. After washing the cells three times, the cells were cultured in 0.2 ml RPMI medium at 37°C. HIV-1 replication was monitored by the quantitation of HIV-1 p24 produced in the culture supernatants for 7 days using the commercially available HIV-1 p24 ELISA kit (Zepto Metrix, Buffalo, NY).

Statistical Analysis. Data were tested for significance using the Student's *t* test by using Prism software (GraphPad Software). The following symbols were used to denote levels of statistical significance: * denotes $P \leq 0.05$, ** denotes $P \leq 0.01$ and *** denotes $P \leq 0.001$.

Results

Monocytes Cultured *in Vitro* in the Presence of IL-4 and IFN-β Require an Additional Source of Stimulation in Order to Survive and Differentiate into Mature DCs. A variety of cytokines/growth factors in varying combinations and concentrations were first evaluated for their potential to induce human monocytes to differentiate into a DC type of morphology *in vitro*. Of these combinations, the most optimal DC type phenotype was observed with the use of IL-4 and IFN-β. However, by 3 days most human monocytes cultured in the presence of IL-4 and IFN-β did not survive due to apoptosis and/or necrosis. Therefore, we attempted to determine whether the addition of exogenous antigens such as KLH, LPS, or inactivated HIV-1 to the cultures would lead to rescue from

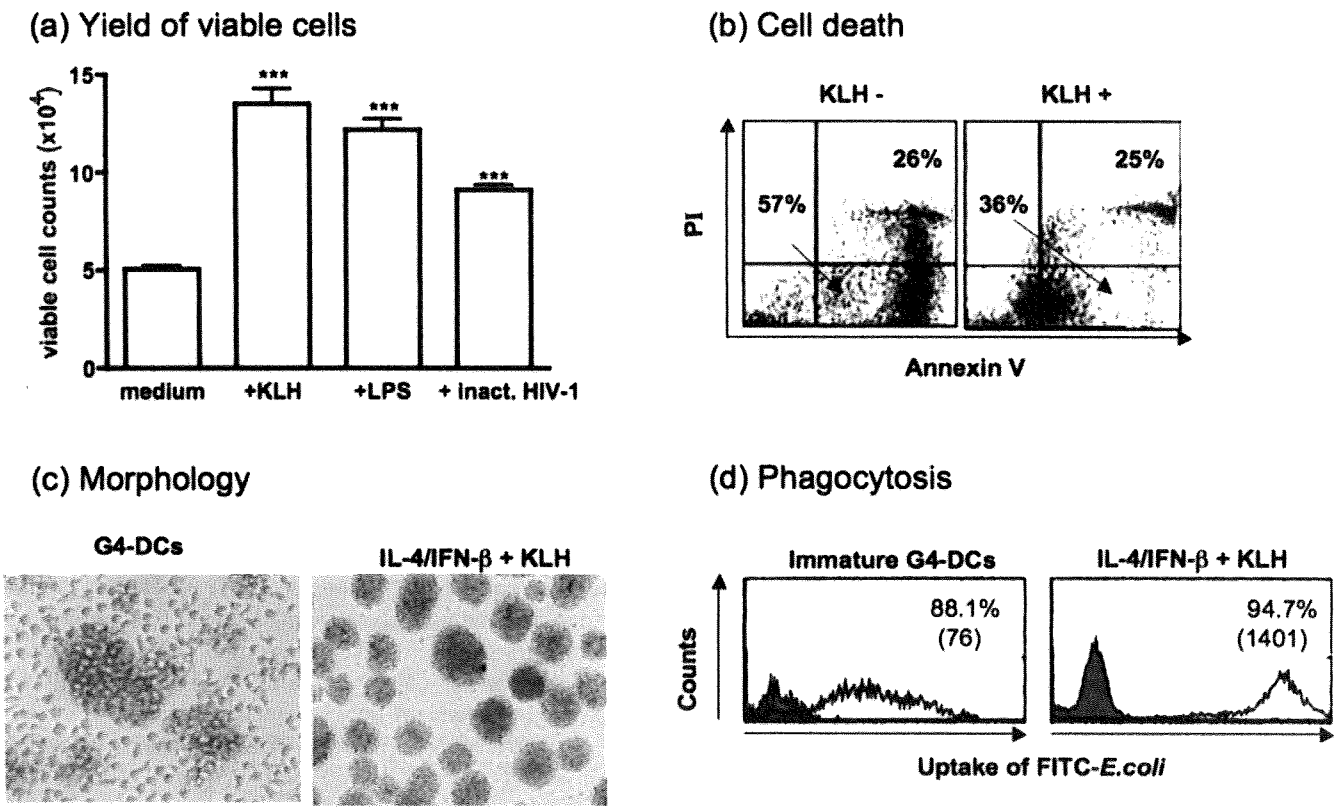

Figure 1. The addition of KLH, LPS, or inactivated HIV-1 promotes the survival of monocytes cultured in media containing IL-4 and IFN-β. $CD14^+$ monocytes purified from PBMCs by a negative selection method (3×10^5 cells/well) were cultured in the presence of IL-4 and IFN-β, followed by the addition of KLH, LPS, or inactivated (inact.) HIV-1 on Day 1 and harvested on Day 3. (a) Yield of total number of viable cells/well. (b) Flow cytometric profile of an aliquot of the monocytes incubated with IL-4 and IFN-β, with and without KLH for 3 days and stained with Annexin V-FITC and PI. (c and d) Comparison of the morphology of and phagocytosis of *E. coli* by the KLH-stimulated monocytes cultured in IL-4 and INF-β (Day 3) and conventional DCs (termed G4-DCs) that had been generated for 7 days from $CD14^+$ monocytes using GM-CSF and IL-4, followed by maturation by IFN-β during last 2 days. The cells were observed under a phase-contrast vertical microscope at an original magnification of ×100. Percent-FITC-positive cells and the mean fluorescence intensity (MFI) are shown in parentheses. Data shown are representative of one of three independent experiments with the standard deviation of <10%. Each experiment utilized three different blood donors and the data depict mean ± SD of the data derived from the three samples.

cell death. As shown in Fig. 1a, the addition of KLH, LPS, or inactivated HIV-1 to the monocyte cultures at a predetermined optimum time interval of Day 1 (see below) led to a 2–3-fold higher increase in the yield of viable cells on Day 3 of culture. A representative profile of annexin V and propidium iodide (PI) staining of monocytes cultured in the presence/absence of KLH is shown in Fig. 1b. As seen, the profile obtained demonstrates that the inclusion of KLH led to marked diminution in the levels of annexin V and PI staining of the *in vitro* cultured cells. Monocytes cultured in parallel in media containing only either IL-4 or IFN-β alone showed poor survival (data not shown). In contrast with conventional DCs derived by culture in media containing IL-4 and GM-CSF followed by further maturation with the addition of IFN-β (hereafter referred to as G4-DCs) which form large aggregates, these IL-4/IFN-β and KLH cultured monocytes not only survived, but also appeared to demonstrate distinct morphology (Fig. 1c). These IL-4/IFN-β and KLH cultured monocytes were shown to not only retain their phagocytic function but appeared to become more efficient as compared with immature G4-DCs, as determined by the uptake of FITC-*E. coli* (Fig. 1d).

As shown in Fig. 2a, IL-4/IFN-β and KLH cultured monocytes expressed high levels of CD83 and CD11c, demonstrating that these cells could be phenotypically defined as mature myeloid DCs (hereafter referred to as 4B-DCs). These KLH-matured 4B-DCs expressed either higher frequencies and/or mean densities of most of the cell surface markers studied except for CD1a. The most marked differences noted were the expression of CCR7 by a significant frequency of 4B-DCs, the universal expression of CD14 and the absence of CD1a by the 4B-DCs. This phenotypic profile was consistently noted and was irrespective of the use of KLH, LPS, or inactivated HIV-1 as a source of antigen stimulation on day 1 (data not shown). Interestingly, a significant frequency of the 4B-DCs was positive for OX40, a marker of activated T cells, and a smaller frequency expressed its ligand OX40L (Fig. 2b). Two-color analysis of OX40/OX40L expression showed that most if not all of the OX40L-expressing 4B-DC population of cells also expressed OX40. It should be

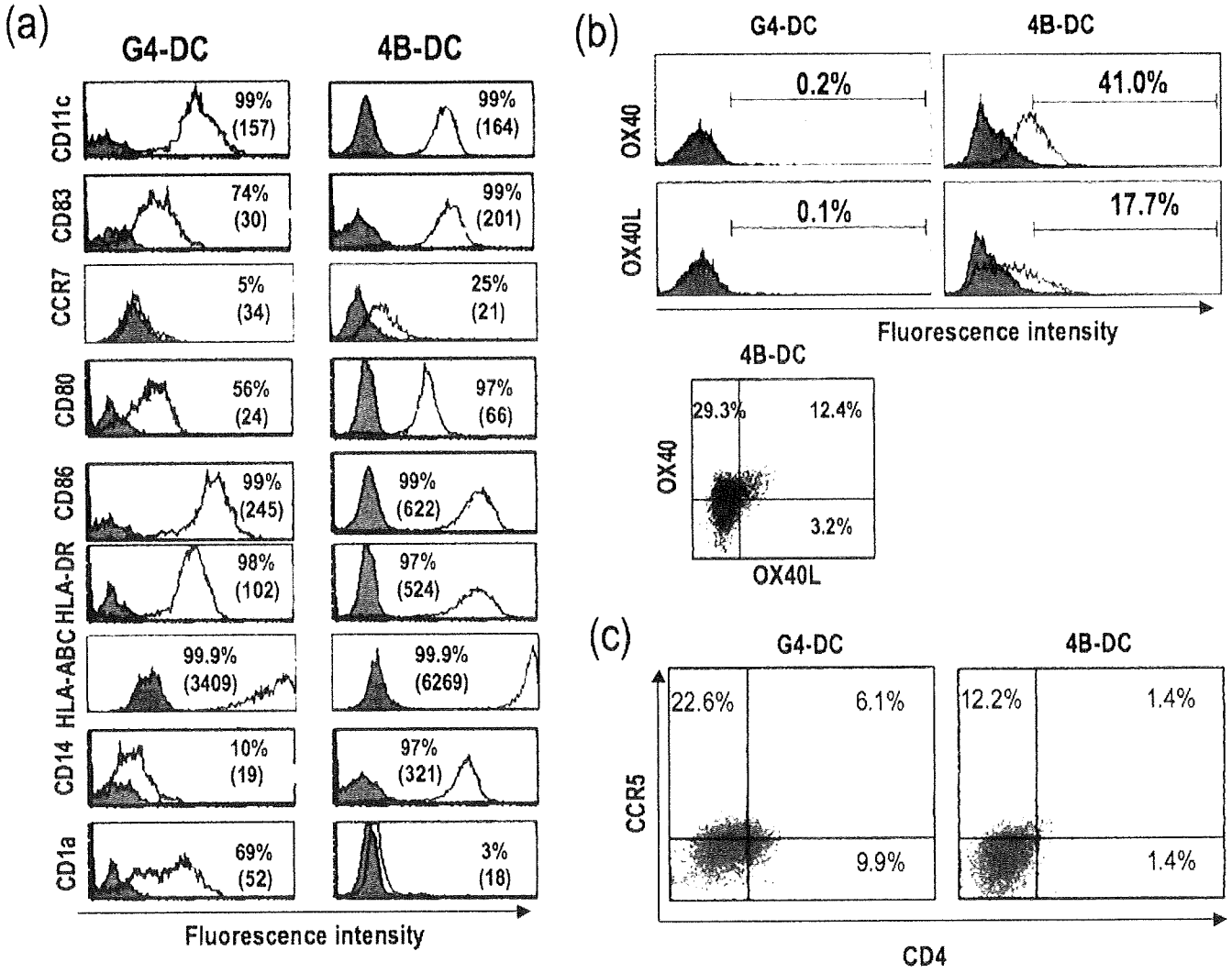

Figure 2. Flow cytometry facilitated phenotypic characterization of IL-4/IFN-β and KLH-cultured monocytes (4B-DCs) and for comparison G4-DCs. (a) 4B-DCs and G4-DCs were examined for cell surface expression of CD11c, CD83, CCR7, CD80, CD86, HLA-DR, HLA-ABC, CD14, and CD1a as described in the Materials and Methods section. Percent-positive cells and MFI in parenthesis are presented. (b) Expression of OX40 and OX40L on these DCs as determined by an indirect and a direct immunofluorescence, upper and lower graph, respectively, are shown. (c) Expression of CD4 and CCR5 as determined using rat anti-human CCR5 T312-FITC and mouse anti-human CD4 OKT-4-Cy5. Each of the data sets shown is representative of three independent experiments with the standard deviation of <10%. Each experiment utilized three different blood donors and the data depict mean ± SD of the data derived from the three samples.

emphasized that the conventional G4-DCs (Fig. 2b) and fresh monocytes (data not shown) were negative for OX40/OX40L, indicating that 4B-DCs acquired OX40 as a result of differentiation from monocytes under the present culture conditions.

The levels of cell surface expression of the HIV-1 receptor CD4 and co-receptor CCR5 are shown in Fig. 2c. Relatively lower levels of CD4 and CCR5 were expressed by 4B-DCs as compared with G4-DCs, which was consistent with the observation that the 4B-DCs were relatively resistant to *in vitro* infection with R5 HIV-1 JR-CSF strain (data not shown).

Optimum Time for the Addition of Antigens and Pathways for 4B-DC Generation. Kinetic studies were carried out in efforts to determine the optimum time that was required for the addition of the antigens such as KLH, LPS, and inactivated HIV-1 for the generation of 4B-DCs. As seen in Fig. 3a, the optimum time for the addition of KLH, LPS, or inactivated HIV-1 was 24 hours. Interestingly, addition of these stimulating agents at the time of initiation of the culture did not result in maximum differentiation, which supports the view that at least a few hours of exposure of the enriched population of monocytes to IL-4 and IFN-β was required for the full differentiation of 4B-DCs.

It was reasoned that because a small amount of LPS (as low as 10 pg/ml) could support 4B-DC generation (data not shown), it was possible that the effects of KLH and inactivated HIV-1 on 4B-DCs maturation was potentially due to contamination of each of these agents with LPS. To exclude this possibility, anti-CD14 neutralizing mAb was

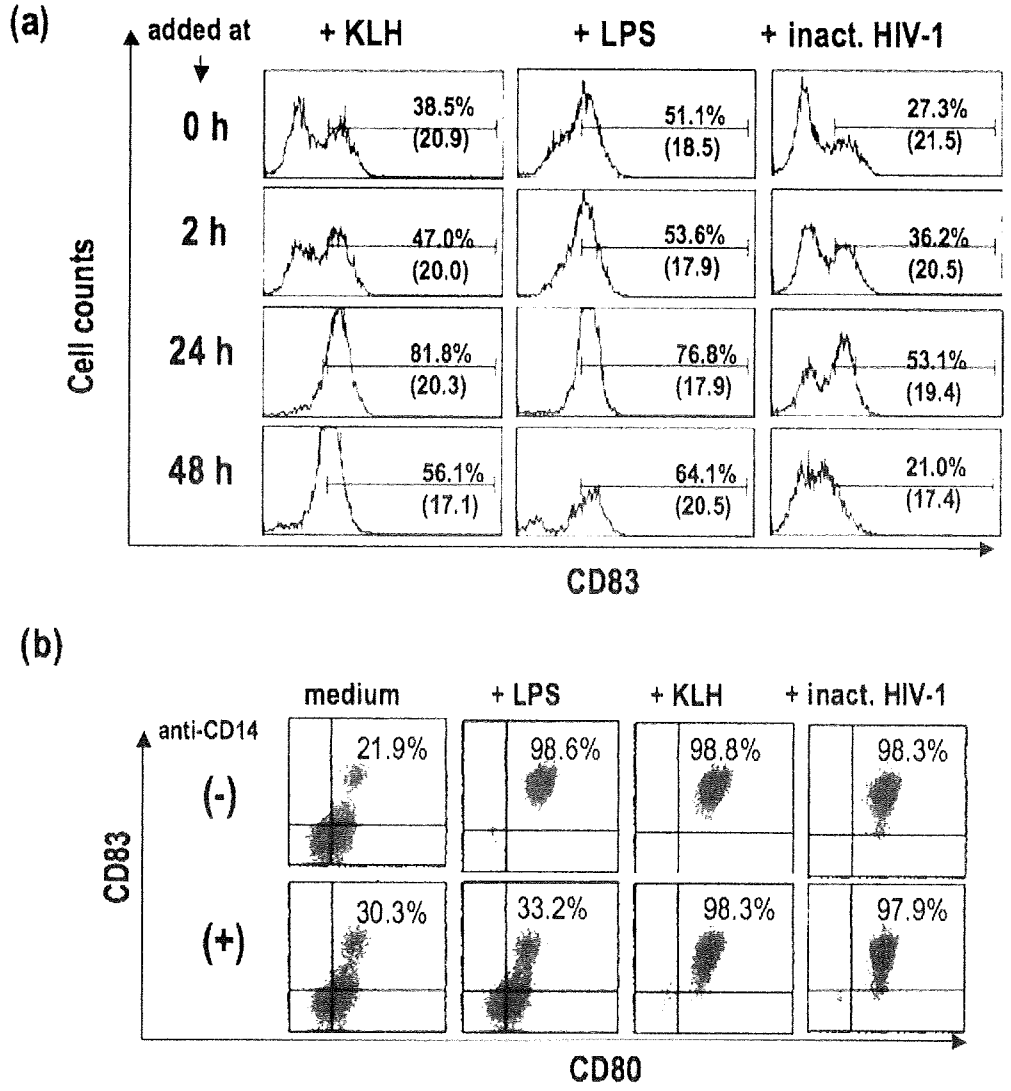

Figure 3. Optimum time for the addition of antigens needed for stimulation and pathways for 4B-DC generation. (a) $CD14^+$ monocytes were cultured in the presence of IL-4 and IFN-β and at indicated times KLH, LPS, or inactivated HIV-1 was added to each culture, and all cultures were harvested on Day 3. An aliquot of the cells were analyzed for the expression of CD83. Percent-positive cells and MFI in parentheses are shown. (b) $CD14^+$ monocytes were cultured in the presence of IFN-β and IL-4 overnight, and then treated with anti-CD14 or for purposes of control an isotype identical mAb (at final 10 μg/ml) at 37°C for 1 hour. Then, LPS, KLH, or inactivated HIV-1 was added to the cultures and cultured for an additional 2 days. The expression of CD83 and CD80 were determined by standard flow cytometry. Data shown are representative of one of three independent experiments with the standard deviation of <10%. Each experiment utilized three different blood donors and the data depict mean ± SD of the data derived from the three samples.

added to the culture to block LPS binding (Fig. 3b). As judged by the expression of CD83 and CD80, the differentiation of 4B-DCs from monocytes with the addition of LPS was completely blocked by the addition of anti-CD14 mAb. However, there appeared to be negligible effects of the addition of the same dose of anti-CD14 mAb on the ability of KLH and inactivated HIV-1 on 4B-DC generation. Therefore, it appears that there are at least two differentiation pathways for 4B-DCs: a CD14-dependent and a CD14-independent pathway under these culture conditions.

Cytokine Production and Naïve $CD4^+$ T Cell Allostimulation by 4B-DCs. In attempts to define functional characteristics of 4B-DCs, the cytokine synthesizing profile and allostimulating properties of these cells were compared with those of G4-DCs. Thus, culture supernatants from the KLH-matured 4B-DCs and the conventional G4-DCs were quantitated by ELISA for levels of IL-12 p70, TNF-α, and IL-10. As seen in Fig. 4a, supernatant fluids from the 4B-DCs produced higher relative levels of IL-12 p70 and TNF-α than the conventional mature G4-DCs. The level of IL-10 production by both 4B-DCs and G4-DCs was low. The results of the cytokine analysis induced by the maturation of 4B-DCs using LPS and inactivated HIV-1 was essentially similar to that of KLH except that there were differences in the relative levels of IL-12 p70 and TNF-α induced by LPS and inactivated HIV-1 (data not shown). Thus, there appeared to be a hierarchy, with LPS inducing the highest levels of

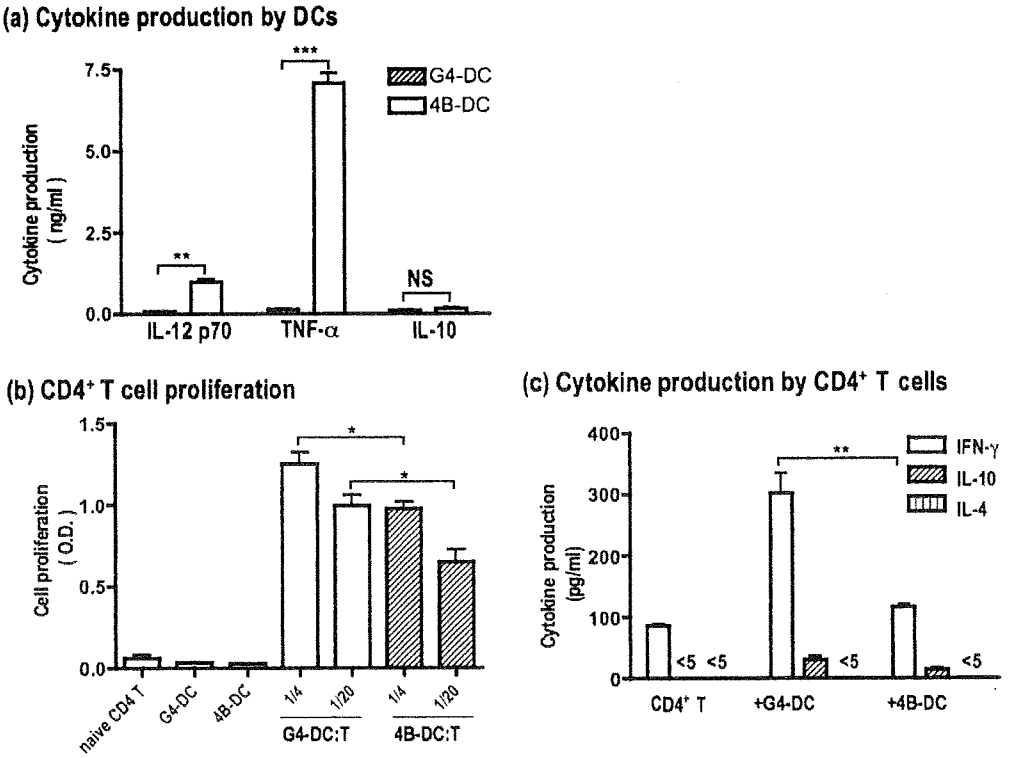

Figure 4. Difference in cytokine production and comparison of the allostimulation potential of naïve $CD4^+$ T cells by 4B-DCs and G4-DCs. 4B-DCs (Day 3) were generated using KLH and conventional G4-DCs (Day 7) were generated by maturation with IFN-β for last 2 days. (a) Supernatants of the two DC cultures were examined for the levels of IL-12 p70, TNF-α, and IL-10 by ELISA. (b) Allogeneic naïve $CD4^+$ T cells were cocultured with either 4B-DCs or G4-DCs for 7 days, and cell proliferation (optical density [O.D.]) of the naïve $CD4^+$ T cells were quantitated by using BrdU-incorporation ELISA kits. (c) Cytokine levels produced in the supernatant fluids by these cocultured cells (Day 7) were determined by ELISA. Data shown are representative of one of three independent experiments with the standard deviation of <10%. Each experiment utilized three different blood donors and the data depict mean ± SD of the data derived from the three samples. NS, not significant.

IL-12 p70 and TNF-α, followed by KLH, and the lowest level induced by inactivated HIV-1.

The allostimulating function of KLH-matured 4B-DCs was next compared with that of G4-DCs using the standard mixed leukocyte reaction (MLR). Purified allogeneic naïve $CD4^+$ T cells were cocultured with either 4B-DCs or G4-DCs at a T to DC ratio of 4:1 or 20:1 for 7 days and the levels of cell proliferation were assessed by BrdU incorporation. As shown in Fig. 4b, the ability of 4B-DCs to induce alloproliferation of the naïve $CD4^+$ T cells was slightly weaker than that of G4-DCs. To determine the cytokine profile of these allostimulated $CD4^+$ T cells induced by 4B-DCs and G4-DCs, the levels of IFN-γ, IL-4, and IL-10 in the culture supernatants of these cultures on day 7 were quantitated by ELISA. As shown in Fig. 4c, the 4B-DC-stimulated T cells secreted lower levels of IFN-γ in comparison to those stimulated with conventional G4-DCs. Production of IL-4 was not detectable (<5 pg/ml) and that of IL-10 was low in these two culture fluids. These data indicate that 4B-DCs were capable of stimulating bulk naïve $CD4^+$ T cell differentiation into Th1-like cells but their potential was lower than conventional G4-DCs.

***In Vitro* Restimulation of 4B-DC-Primed $CD4^+$ T Cells.** Because 4B-DCs were less effective than G4-DCs in induction of $CD4^+$ T cell proliferation as described above, we reasoned that this difference could be due to the differential activation of Tregs by the former. However, these $CD4^+$ T cells allo-activated by either 4B-DCs or G4-DCs failed to show detectable levels of Treg activity. Thus as seen in Fig. 5a, Experiment 1, the responder $CD4^+$ T cells cultured in the absence (control) or presence of allo-4B-DC-primed $CD4^+$ T cells, as well as those primed with allo-G4-DCs (at cell to cell ratio of 1:1) gave the same CFSE profile, indicating that the Treg frequency in the $CD4^+$ T cells primed either with 4B-DCs or G4-DCs was either absent and/or undetectable under these culture conditions. To provide for a more sensitive assay for the detection of potential Tregs, these alloprimed $CD4^+$ T cells were restimulated by incubation with immobilized OKT-3 mAb together with soluble anti-CD28 mAb for 2 days and then assayed for Treg activity and IL-10 production as described in the Methods section. Interestingly, $CD4^+$ T cells from both the 4B-DCs and G4-DCs primed and *in vitro* expanded cells showed Treg activity at a responder to Treg cell ratio of 1:1 as shown by marked inhibition of autologous naïve $CD4^+$ T cell proliferation (Fig. 5a, Experiment 2), indicating that there is no significant difference in Treg-inducing activity between 4B-DCs and G4-DCs. However, as seen in Fig. 5b the 4B-DC-primed and restimulated $CD4^+$ T cells produced higher levels of IL-10 and lower levels of IFN-γ

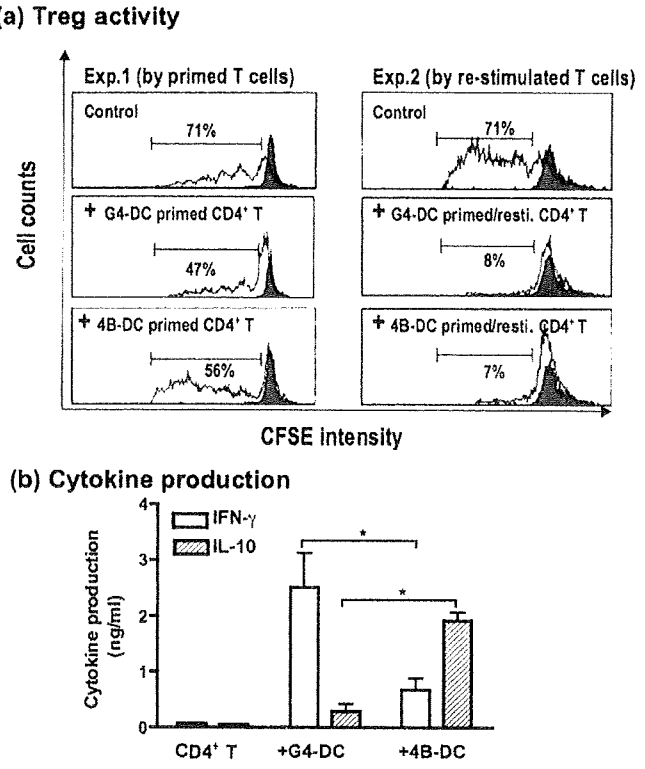

Figure 5. Analysis of Treg generation by coculture with 4B-DCs and the synthesis of IL-10 by restimulated $CD4^+$ T cells. Allogeneic KLH-matured 4B-DC- or conventional G4-DC-primed $CD4^+$ T cells as shown in Fig. 4b, or those cells after restimulation were examined for cytokine production and Treg activity. (a) 4B-DC- or G4-DC-primed $CD4^+$ T cells, and those restimulated with anti-CD3/CD28 mAbs were added to CFSE-labeled autologous naïve $CD4^+$ T cells cultures at a 1:1 ratio. Then soluble OKT-3 and autologous monocytes were added to the cultures. After 3 days, proliferation of the $CD4^+$ T cells was analyzed by flow cytometry. (b) Cytokine production by the restimulated culture supernatants was quantitated by ELISA. Data shown are representative of one of three independent experiments with the standard deviation of <10%. Each experiment utilized three different blood donors and the data depict mean ± SD of the data derived from the three samples.

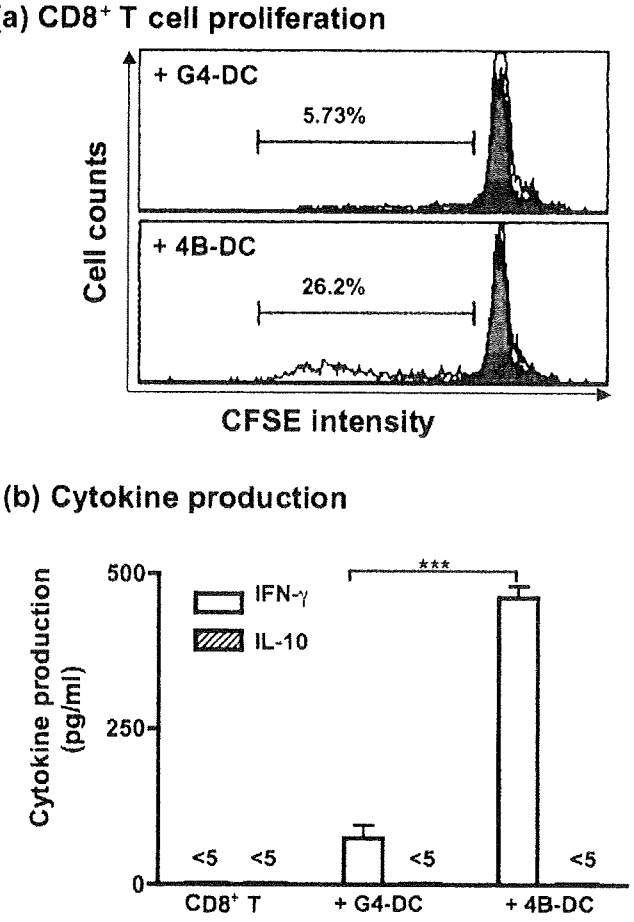

Figure 6. Stimulation of $CD8^+$ T cells with 4B-DCs. CFSE-labeled purified $CD8^+$ T cells were cocultured with allogeneic KLH-matured 4B-DCs or G4-DCs at T to DC ratio of 4:1 in RPMI medium containing IL-2 (20 U /ml) in 96 well U-bottom plate for 6 days. (a) Proliferation of the CFSE-labeled $CD8^+$ T cells was assayed by flow cytometry. The frequency of proliferating cells of is shown. (b) IFN-γ production by non-labeled $CD8^+$ cells in the culture supernatants were quantitated by ELISA. Data shown are representative of one of three independent experiments with the standard deviation of <10%. Each experiment utilized three different blood donors and the data depict mean ± SD of the data derived from the three samples.

than those that were G4-DC-primed/restimulated, showing a somewhat difference between the two DC populations in determination of T cell differentiation.

$CD8^+$ T Cell Stimulation by 4B-DCs. Finally, the biological effects of 4B-DCs on $CD8^+$ T cells were examined by standard MLR. Highly purified (>95%) $CD8^+$ T cells that were labeled with CFSE were cocultured with allogeneic 4B-DCs or G4-DCs at a ratio of 4:1 (responder to stimulator) for 6 days. As shown in Fig. 6a, 4B-DC-induced alloproliferation of $CD8^+$ T cells was more effectively than those induced by G4-DCs although the relative proliferative potential of these DC preparations for allogeneic $CD8^+$ T cells was weaker than that noted above for $CD4^+$ T cells. Supernatant fluids from such cultures were also examined for levels of IFN-γ and IL-10. As seen in Fig. 6b, the allo-4B-DC-stimulated $CD8^+$ T cells synthesized significantly more IFN-γ than those stimulated with G4-DCs. IL-10 was not detected in these culture supernatant fluids. These data suggest that 4B-DCs were committed to stimulate $CD8^+$ T cells rather than $CD4^+$ T cells, which was in contrast to the case of the G4-DCs.

Discussion

The present study was conducted in efforts to define *in vitro* methodologies that could potentially hasten the *in vitro* maturation of myeloid DCs from human monocytes. Results of our studies show that indeed *in vitro* culture of highly enriched population of $CD14^+$ human monocytes in the presence of IL-4 and IFN-γ for 1 day, followed by the addition of KLH, LPS, or AT-2-inactivated HIV-1 IIIB strain for 2 days, led to the generation of mature and functional myeloid DCs. These 4B-DCs displayed several distinct phenotypes from conventional DCs (Figs. 1 and 2) and from those reported as rapidly-induced DCs that were derived by using a cocktail of IL-6, IL-1β, TNF-α, and PGE_2 (14, 15). The 4B-DCs expressed 3–6-fold higher

levels of CD83, CD80, CD86, HLA class-I, and class-II antigens than mature conventional G4-DCs from the same donors. In contrast to conventional G4-DCs, 4B-DCs expressed higher relative levels of CD14 but not CD1a which is a typical phenotype for precursor Langerhans cells (29), suggesting that 4B-DCs are sensitive to LPS stimulation but deficient in presentation of lipid antigens to T cells (30).

Another apparent phenotypic difference between 4B-DCs and G4-DCs was that 4B-DCs expressed the T cell activation marker OX40 under the present culture conditions. Although OX40L has been reported to be induced on DCs by treatment with CD40L or thymic stromal lymphopoietin (31, 32), to the best of our knowledge, this is the first study to report the expression of OX40 on human DCs. Our data suggest that the OX40 was endogenously induced on DCs and not transferred from contaminating activated $OX40^+$ T cells (33) because the cultures were prescreened for such contaminating cells and OX40 was detected on 4B-DCs generated in the presence of anti-OX40 mAb (W4–54) that has been previously shown to block the passive transfer of OX40 (27). As it has been previously suggested that the interaction between OX40 and OX40L on T cells promotes survival of the T cells (34), because some of 4B-DCs were positive for OX40L, it is thus possible that the dual expressions of these antigens on 4B-DCs may have been involved in the control of survival and/or function of these cells through an autocrine and/or paracrine pathway. The mechanism of OX40 induction and its biological function remains to be determined, and experiments using anti-OX40 agonistic mAbs and soluble recombinant OX40L are currently in progress.

Another difference noted between 4B-DCs and conventional G4-DCs was that the 4B-DCs were nonadherent to the bottom of the plastic culture vessels, formed clusters, and formed large clumps in culture in 3 days. This morphology of 4B-DCs was very distinct from that of so-called typical "dendritic" cell, suggesting differences in the expression patterns of adhesion-related molecules which may include DC-SIGN, ICAM-3, extracellular matrix proteins, or their receptors.

The requirement for the addition of KLH, LPS, or inactivated HIV-1, as an additional stimulant after short-time culture of $CD14^+$ monocytes for survival and differentiation of 4B-DCs remains to be determined, and is a subject of studies in progress. Some of these data indicate that LPS is likely activating the progenitor cells via both the CD14 and the TLR4-mediated signal pathway (35). On the other hand, KLH appears to mediate its effect via the mannose receptor-mediated pathway (36), and HIV-1-induced maturation likely involves the TLR7/TLR8 pathways. The latter data is supported by the finding that single strand viral RNAs have the potential to signal via the TLR7/TLR8 pathways (37). Because type-I IFN is known to skew the differentiation of monocytes into TLR7-expressing DCs (16), the monocytes cultured in the present media containing IFN-β and IL-4 for 1 day might acquire TLR7 during this initial culture period. Our preliminary studies showed that CpG, the ligand of TLR9, could not generate mature 4B-DCs (data not shown), indicating that TLR9 pathway is not likely involved. It will be of interest to further examine which other TLRs can support 4B-DC generation.

Experiments on cytokine production patterns showed that 4B-DCs produced higher relative levels of IL-12 p70 and TNF-α than G4-DCs, and that IL-10 was low in supernatant fluids from both the cultures. This pattern is in contrast to those of the other type-I IFN-derived DCs in the presence of GM-CSF that produced less IL-12 than conventional DCs (16, 17). However, like the other type-I IFN-derived DCs (38), 4B-DCs showed reduced potential to induce alloproliferation of naïve $CD4^+$ T cells and the synthesis of IFN-γ, as compared with G4-DCs. One possible reason for this may be related to the induction or stimulation of Tregs as reported by Carbonneil *et al.* (38) However, we could not detect any Tregs activity in these primary allo-4B-DC-stimulated $CD4^+$ T cells. Nevertheless, restimulation of the 4B-DC-primed $CD4^+$ T cells resulted in production of higher levels of IL-10 and less levels of IFN-γ than those primed with G4-DCs (Fig. 5). Thus, it is still possible that endogenously produced IL-10 might be involved in the low proliferation of the responder naïve $CD4^+$ T cells stimulated allo-4B-DCs. Another possibility is that 4B-DCs had a shorter life span than G4-DCs (data not shown), which may be not enough for continuous stimulation of $CD4^+$ T cells during the later stages.

There have been several studies performed aimed at exploring the potential beneficial effects of type-I IFN on monocyte-derived DCs in reference to immune protection against viral infections. Carbonneil *et al.* (20) reported that IFN-α together with GM-CSF induced monocytes to differentiate into functional and HIV-resistant DCs that are capable of inducing potent HIV-specific $CD8^+$ T cell responses. Similarly, Santodonato *et al.* (39) demonstrated that 3-day DCs generated from monocytes in the presence of IFN-α and GM-CSF stimulated Epstein-Barr virus-specific $CD8^+$ T cell responses. Thus it seems likely that DCs induced in the presence of type-I IFN, which express high levels of MHC class-I/II antigens, may favor $CD8^+$ T rather than $CD4^+$ T cell induction and have the potential to be highly effective against viral infections. Indeed, our present data showed that 4B-CDs were more potent to stimulate allogeneic bulk $CD8^+$ T cells than G4-DCs. Another benefit of type-I IFN-induced or -treated DCs may be that they are resistant to productive infection with viruses including HIV-1 (20), influenza virus (40), and even Ebola virus (41), which may be applicable in clinical DC-based immunotherapy trials for such virally infected patients. As indicated herein, DC-based immunotherapy platforms continue to be utilized in a variety of clinical settings meant to either induce and augment pro-inflammatory immune responses (in the case of vaccines against infectious agents), modulate immune responses (such as in patients with autoimmune

diseases), and/or suppress immune responses (such as in organ/tissue allotransplantation). Thus, care needs to be taken in the use of proper sets of DCs and their biological characteristics thoroughly tested in animal models prior to their use in human studies. In particular, there is a need for making sure that utilization of DC-based immunotherapy does not inadvertently initiate an autoimmune response.

Studies are in progress to explore whether the present 4B-DCs are able to induce HIV-1-specific $CD8^+$ and $CD4^+$ T cell responses *in vitro* and *in vivo* using our hu-PBL-SCID mouse model (9).

We thank the National Institutes of Health AIDS Research and Reference Reagent Program for supplying IL-2.

1. Banchereau J, Briere F, Caux C, Davoust J, Lebecque S, Liu YJ, Pulendran B, Palucka K. Immunobiology of dendritic cells. Annu Rev Immunol 18:767–811, 2000.
2. Steinman RM, Hemmi H. Dendritic cells: translating innate to adaptive immunity. Curr Top Microbiol Immunol 311:17–58, 2006.
3. Sallusto F, Lanzavecchia A. Understanding dendritic cell and T-lymphocyte traffic through the analysis of chemokine receptor expression. Immunol Rev 177:134–140, 2000.
4. Reddy ST, Swartz MA, Hubbell JA. Targeting dendritic cells with biomaterials: developing the next generation of vaccines. Trends Immunol 27:573–579, 2006.
5. Gilboa E. DC-based cancer vaccines. J Clin Invest 117:1195–1203, 2007.
6. Lu W, Wu X, Lu Y, Guo W, Andrieu JM. Therapeutic dendritic-cell vaccine for simian AIDS. Nat Med 9:27–32, 2003.
7. Connolly NC, Colleton BA, Rinaldo CR. Treating HIV-1 infection with dendritic cells. Curr Opin Mol Ther 9:353–363, 2007.
8. Lapenta C, Santini SM, Logozzi M, Spada M, Andreotti M, Di Pucchio T, Parlato S, Belardelli F. Potent immune response against HIV-1 and protection from virus challenge in hu-PBL-SCID mice immunized with inactivated virus-pulsed dendritic cells generated in the presence of IFN-alpha. J Exp Med 198:361–367, 2003.
9. Yoshida A, Tanaka R, Murakami T, Takahashi Y, Koyanagi Y, Nakamura M, Ito M, Yamamoto N, Tanaka Y. Induction of protective immune responses against R5 human immunodeficiency virus type 1 (HIV-1) infection in hu-PBL-SCID mice by intrasplenic immunization with HIV-1-pulsed dendritic cells: possible involvement of a novel factor of human $CD4^+$ T-cell origin. J Virol 77:8719–8728, 2003.
10. Tuyaerts S, Aerts JL, Corthals J, Neyns B, Heirman C, Breckpot K, Thielemans K, Bonehill A. Current approaches in dendritic cell generation and future implications for cancer immunotherapy. Cancer Immunol Immunother 56:1513–1537, 2007.
11. Yates SF, Paterson AM, Nolan KF, Cobbold SP, Saunders NJ, Waldmann H, Fairchild PJ. Induction of regulatory T cells and dominant tolerance by dendritic cells incapable of full activation. J Immunol 179:967–976, 2007.
12. Santini SM, Di Pucchio T, Lapenta C, Parlato S, Logozzi M, Belardelli F. A new type I IFN-mediated pathway for the rapid differentiation of monocytes into highly active dendritic cells. Stem Cells 21: 357–362, 2003.
13. Santini SM, Lapenta C, Logozzi M, Parlato S, Spada M, Di Pucchio T, Belardelli F. Type I interferon as a powerful adjuvant for monocyte-derived dendritic cell development and activity in vitro and in Hu-PBL-SCID mice. J Exp Med 191:1777–1788, 2000.
14. Dauer M, Schad K, Herten J, Junkmann J, Bauer C, Kiefl R, Endres S, Eigler A. FastDC derived from human monocytes within 48 h effectively prime tumor antigen-specific cytotoxic T cells. J Immunol Methods 302:145–155, 2005.
15. Obermaier B, Dauer M, Herten J, Schad K, Endres S, Eigler A. Development of a new protocol for 2-day generation of mature dendritic cells from human monocytes. Biol Proced Online 5:197–203, 2003.
16. Mohty M, Vialle-Castellano A, Nunes JA, Isnardon D, Olive D, Gaugler B. IFN-alpha skews monocyte differentiation into Toll-like receptor 7-expressing dendritic cells with potent functional activities. J Immunol 171:3385–3393, 2003.
17. Dauer M, Pohl K, Obermaier B, Meskendahl T, Robe J, Schnurr M, Endres S, Eigler A. Interferon-alpha disables dendritic cell precursors: dendritic cells derived from interferon-alpha-treated monocytes are defective in maturation and T-cell stimulation. Immunology 110:38–47, 2003.
18. McRae BL, Nagai T, Semnani RT, van Seventer JM, van Seventer GA. Interferon-alpha and -beta inhibit the in vitro differentiation of immunocompetent human dendritic cells from $CD14^+$ precursors. Blood 96:210–217, 2000.
19. Paquette RL, Hsu NC, Kiertscher SM, Park AN, Tran L, Roth MD, Glaspy JA. Interferon-alpha and granulocyte-macrophage colony-stimulating factor differentiate peripheral blood monocytes into potent antigen-presenting cells. J Leukoc Biol 64:358–367, 1998.
20. Carbonneil C, Aouba A, Burgard M, Cardinaud S, Rouzioux C, Langlade-Demoyen P, Weiss L. Dendritic cells generated in the presence of granulocyte-macrophage colony-stimulating factor and IFN-alpha are potent inducers of HIV-specific CD8 T cells. AIDS 17: 1731–1740, 2003.
21. Sallusto F, Lanzavecchia A. Efficient presentation of soluble antigen by cultured human dendritic cells is maintained by granulocyte/macrophage colony-stimulating factor plus interleukin 4 and downregulated by tumor necrosis factor alpha. J Exp Med 179:1109–1118, 1994.
22. Roy KC, Bandyopadhyay G, Rakshit S, Ray M, Bandyopadhyay S. IL-4 alone without the involvement of GM-CSF transforms human peripheral blood monocytes to a CD1a(dim), CD83(+) myeloid dendritic cell subset. J Cell Sci 117:3435–3445, 2004.
23. Tanaka R, Yoshida A, Murakami T, Baba E, Lichtenfeld J, Omori T, Kimura T, Tsurutani N, Fujii N, Wang ZX, Peiper SC, Yamamoto N, Tanaka Y. Unique monoclonal antibody recognizing the third extracellular loop of CXCR4 induces lymphocyte agglutination and enhances human immunodeficiency virus type 1-mediated syncytium formation and productive infection. J Virol 75:11534–11543, 2001.
24. Takahashi Y, Tanaka Y, Yamashita A, Koyanagi Y, Nakamura M, Yamamoto N. OX40 stimulation by gp34/OX40 ligand enhances productive human immunodeficiency virus type 1 infection. J Virol 75: 6748–6757, 2001.
25. Tanaka Y, Inoi T, Tozawa H, Yamamoto N, Hinuma Y. A glycoprotein antigen detected with new monoclonal antibodies on the surface of human lymphocytes infected with human T-cell leukemia virus type-I (HTLV-I). Int J Cancer 36:549–555, 1985.
26. Tanaka Y, Yoshida A, Tozawa H, Shida H, Nyunoya H, Shimotohno K. Production of a recombinant human T-cell leukemia virus type-I trans-activator (tax1) antigen and its utilization for generation of monoclonal antibodies against various epitopes on the tax1 antigen. Int J Cancer 48:623–630, 1991.
27. Kondo K, Okuma K, Tanaka R, Zhang LF, Kodama A, Takahashi Y, Yamamoto N, Ansari AA, Tanaka Y. Requirements for the functional expression of OX40 ligand on human activated $CD4^+$ and $CD8^+$ T cells. Hum Immunol 68:563–571, 2007.
28. Nimura F, Zhang LF, Okuma K, Tanaka R, Sunakawa H, Yamamoto N, Tanaka Y. Cross-linking cell surface chemokine receptors leads to isolation, activation, and differentiation of monocytes into potent dendritic cells. Exp Biol Med (Maywood) 231:431–443, 2006.
29. Morelli AE, Rubin JP, Erdos G, Tkacheva OA, Mathers AR, Zahorchak AF, Thomson AW, Falo LD, Jr., Larregina AT. $CD4^+$ T cell responses

elicited by different subsets of human skin migratory dendritic cells. J Immunol 175:7905–7915, 2005.
30. Porcelli SA, Modlin RL. The CD1 system: antigen-presenting molecules for T cell recognition of lipids and glycolipids. Annu Rev Immunol 17:297–329, 1999.
31. Ohshima Y, Tanaka Y, Tozawa H, Takahashi Y, Maliszewski C, Delespesse G. Expression and function of OX40 ligand on human dendritic cells. J Immunol 159:3838–3848, 1997.
32. Ito T, Wang YH, Duramad O, Hori T, Delespesse GJ, Watanabe N, Qin FX, Yao Z, Cao W, Liu YJ. TSLP-activated dendritic cells induce an inflammatory T helper type 2 cell response through OX40 ligand. J Exp Med 202:1213–1223, 2005.
33. Baba E, Takahashi Y, Lichtenfeld J, Tanaka R, Yoshida A, Sugamura K, Yamamoto N, Tanaka Y. Functional CD4 T cells after intercellular molecular transfer of OX40 ligand. J Immunol 167:875–883, 2001.
34. Soroosh P, Ine S, Sugamura K, Ishii N. OX40-OX40 ligand interaction through T cell-T cell contact contributes to CD4 T cell longevity. J Immunol 176:5975–5987, 2006.
35. Takeda K, Kaisho T, Akira S. Toll-like receptors. Annu Rev Immunol 21:335–376, 2003.
36. Presicce P, Taddeo A, Conti A, Villa ML, Bella SD. Keyhole limpet hemocyanin induces the activation and maturation of human dendritic cells through the involvement of mannose receptor. Mol Immunol 45: 1136–1145, 2008.
37. Heil F, Hemmi H, Hochrein H, Ampenberger F, Kirschning C, Akira S, Lipford G, Wagner H, Bauer S. Species-specific recognition of single-stranded RNA via toll-like receptor 7 and 8. Science 303:1526–1529, 2004.
38. Carbonneil C, Saidi H, Donkova-Petrini V, Weiss L. Dendritic cells generated in the presence of interferon-alpha stimulate allogeneic $CD4^+$ T-cell proliferation: modulation by autocrine IL-10, enhanced T-cell apoptosis and T regulatory type 1 cells. Int Immunol 16:1037–1052, 2004.
39. Santodonato L, D'Agostino G, Nisini R, Mariotti S, Monque DM, Spada M, Lattanzi L, Perrone MP, Andreotti M, Belardelli F, Ferrantini M. Monocyte-derived dendritic cells generated after a short-term culture with IFN-alpha and granulocyte-macrophage colony-stimulating factor stimulate a potent Epstein-Barr virus-specific $CD8^+$ T cell response. J Immunol 170:5195–5202, 2003.
40. Thitithanyanont A, Engering A, Ekchariyawat P, Wiboon-ut S, Limsalakpetch A, Yongvanitchit K, Kum-Arb U, Kanchongkittiphon W, Utaisincharoen P, Sirisinha S, Puthavathana P, Fukuda MM, Pichyangkul S. High susceptibility of human dendritic cells to avian influenza H5N1 virus infection and protection by IFN-alpha and TLR ligands. J Immunol 179:5220–5227, 2007.
41. Mahanty S, Hutchinson K, Agarwal S, McRae M, Rollin PE, Pulendran B. Cutting edge: impairment of dendritic cells and adaptive immunity by Ebola and Lassa viruses. J Immunol 170:2797–2801, 2003.

Available online at www.sciencedirect.com
ScienceDirect
Virology 375 (2008) 130–140
VIROLOGY
www.elsevier.com/locate/yviro

Ezrin, Radixin, and Moesin (ERM) proteins function as pleiotropic regulators of human immunodeficiency virus type 1 infection

Yoshinao Kubo [a,*], Hiroaki Yoshii [a], Haruka Kamiyama [a], Chika Tominaga [a], Yuetsu Tanaka [b], Hironori Sato [a,c], Naoki Yamamoto [a,d]

[a] Department of AIDS Research, Institute of Tropical Medicine, Nagasaki University, Nagasaki, National Institute of Infectious Diseases, Tokyo, Japan
[b] Department of Immunology, University of the Ryukyus, Okinawa, National Institute of Infectious Diseases, Tokyo, Japan
[c] Laboratory of Viral Genomics, Center for Pathogen Genomics, National Institute of Infectious Diseases, Tokyo, Japan
[d] AIDS Research Center, National Institute of Infectious Diseases, Tokyo, Japan

Received 5 November 2007; returned to author for revision 21 November 2007; accepted 30 January 2008
Available online 4 March 2008

Abstract

Ezrin, radixin, and moesin (ERM) proteins supply functional linkage between integral membrane proteins and cytoskeleton in mammalian cells to regulate membrane protein dynamisms and cytoskeleton rearrangement. To assess potential role of the ERM proteins in HIV-1 lifecycle, we examined if suppression of ERM function in human cells expressing HIV-1 infection receptors influences HIV-1 envelope (Env)-mediated HIV-1-vector transduction and cell–cell fusion. Expression of an ezrin dominant negative mutant or knockdown of ezrin, radixin, or moesin with siRNA uniformly decreased transduction titers of HIV-1 vectors having X4-tropic Env. In contrast, transduction titers of R5-tropic Env HIV-1 vectors were decreased only by radixin knockdown: ezrin knockdown had no detectable effects and moesin knockdown rather increased transduction titer. Each of the ERM suppressions had no detectable effects on cell surface expression of CD4, CCR5, and CXCR4 or VSV-Env-mediated HIV-1 vector transductions. Finally, the individual knockdown of ERM mRNAs uniformly decreased efficiency of cell–cell fusion mediated by X4- or R5-tropic Env and HIV-1 infection receptors. These results suggest that (i) the ERM proteins function as positive regulators of infection by X4-tropic HIV-1, (ii) moesin additionally functions as a negative regulator of R5-tropic HIV-1 virus infection at the early step(s) after the membrane fusion, and (iii) receptor protein dynamisms are regulated differently in R5- and X4-tropic HIV-1 infections.

Keywords: HIV-1; Ezrin; Radixin; Moesin

Introduction

Human immunodeficiency virus type 1 (HIV-1) enters into host cells by fusion between viral envelope and host cell membrane following the binding of HIV-1 envelope glycoprotein (Env) to the cell surface receptors, CD4 and co-receptor (CXCR4 or CCR5). The HIV-1 Env glycoprotein is synthesized as a precursor polyprotein, and cleaved to surface (SU) and transmembrane (TM) subunits by a cellular protease. The conformational change of SU subunit by its interaction with CD4 triggers the formation and exposure of the co-receptor binding domain. The binding of SU subunit to the co-receptor molecule activates the membrane fusion capability of the viral TM subunit required for the HIV-1 entry into host cells.

After the HIV-1 Env protein binds to host cells, the HIV-1 infection receptors are clustered (Jolly and Sattentau, 2005; Nguyen et al., 2005; Viard et al., 2002). The receptor clustering requires cytoskeletal functions (Iyengar et al., 1998; Jolly et al., 2004; Kizhatil and Albritton, 1997; Lehmann et al., 2005; Pontow et al., 2004; Steffens and Hope, 2003). This results in multiple interactions between the viral Env proteins and the host receptor molecules on the interacting site between host cell and virion (Jimenez-Baranda et al., 2007; Platt et al., 1998). Although accumulating evidence indicates that the cytoskeleton-dependent clustering of infection receptors are essential for

* Corresponding author. Department of AIDS Research, Institute of Tropical Medicine, Nagasaki University, 1-12-4 Sakamoto, Nagasaki, Japan 852-8523. Fax: +81 95 849 7805.
E-mail address: yoshinao@net.nagasaki-u.ac.jp (Y. Kubo).

0042-6822/$ - see front matter © 2008 Elsevier Inc. All rights reserved.
doi:10.1016/j.virol.2008.01.047

efficient membrane fusion and subsequent entry of HIV-1 into the target cells, there is no evidence that the receptor proteins, CD4, CXCR4, and CCR5, directly bind to the cytoskeleton. This suggests that some linker molecules between the receptor and cytoskeleton is involved in the HIV-1 entry.

Ezrin, radixin, and moesin are the cytosolic proteins called ERM family that supplies functional linkage between integral membrane proteins and cytoskeleton (Algrain et al., 1993; Fievet et al., 2006; Tsukita et al., 1997). They are highly homologous each other, sharing about 70–80% amino acid identity. The ERM plays key roles in cell morphogenesis and communication via regulating membrane protein dynamisms and cytoskeleton rearrangement (Tsukita et al., 1997). The ERM, particularly ezrin, is important for reconstructing cell-surface architecture during T cell activation (Das et al., 2002; Faure et al., 2004; Gupta et al., 2006; Roumier et al., 2001). Despite the general similarity in structure and function, individual function of the three proteins appears to be specialized (Doi et al., 1999; Kikuchi et al., 2002; Saotome et al., 2004; Takeuchi et al., 1994). Ezrin is crucial for formation of local architecture, called immunological synapse, at the contact site of antigen-presenting and T cells (Gupta et al., 2006; Roumier et al., 2001). Dephosphorylation and relocation of

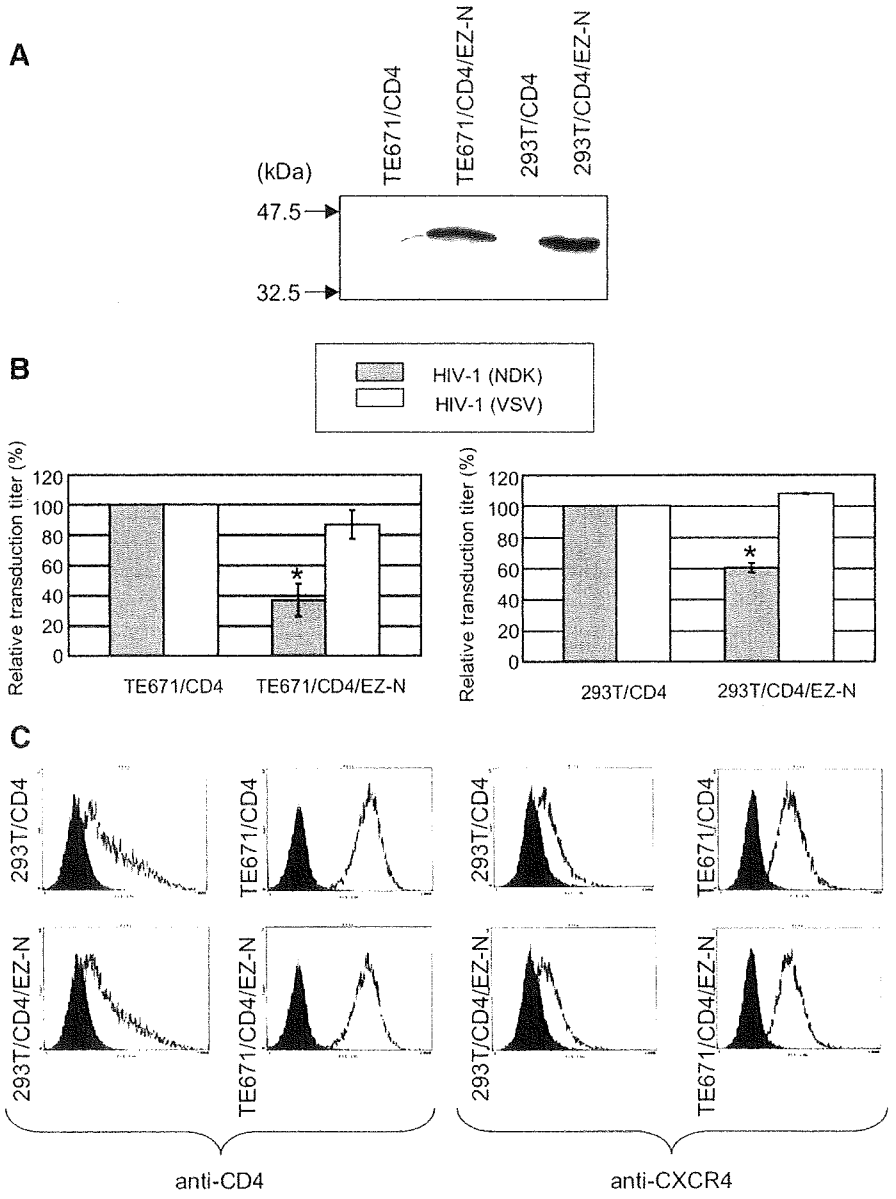

Fig. 1. Effect of ezrin dominant negative mutant on vector transduction. Panel A. Cell lysates prepared from cells expressing the VSV-G epitope-tagged ezrin dominant negative mutant (EZ-N) were subjected to Western immunoblotting using the anti-VSV-G epitope antibody. Molecular size markers are indicated in left side of the panel. Panel B. Transduction titers of the HIV-1 vector having VSV-G (open bar) or NDK HIV-1 Env (closed bar) protein were measured in the control and EZ-N-expressing cells. Relative values to the titer in the control cells are shown. Three independent experiments were performed. Error bars indicate standard deviations. Panel C. Cell surface expression of CD4 and CXCR4 in the control and the EZ-N-expressing cells was analysed by FACS. Closed areas indicate cells stained without the first antibody. Open areas indicate cells stained with the anti-CD4 or anti-CXCR4 antibody.

ezrin trigger transient uncoupling of lipid rafts or plasma membrane from the actin cytoskeleton, which presumably increases lipid raft dynamics and T cell receptor clustering (Gupta et al., 2006). The immunological synapse contains CD4 and CXCR4 (Roumier et al., 2001), the HIV-1 infection receptors, and its formation requires cytoskeleton rearrangement (Das et al., 2002). In addition, the HIV-1 receptors have been reported to co-localize with ezrin (Steffens and Hope, 2003).

In this study, we examined potential roles of the ERM proteins in the HIV-1 infection. We prepared HIV-1-susceptible human cells in which function or expression of the ERM family proteins were suppressed by either ezrin dominant negative mutant (Algrain et al., 1993) or by RNA interference technique (Rana, 2007). Suppression of individual ERM in the target cells yielded distinct effects on HIV-1 vector transductions mediated by the X4- and R5-tropic Env proteins. The ERM suppressions uniformly inhibited cell–cell fusion mediated by the X4- and R5-tropic envelope proteins. Our findings provide for the first time the evidence that the ERM family proteins function as pleiotropic regulators of HIV-1 infection.

Results

Ezrin dominant negative mutant inhibits X4-tropic HIV-1 vector infection

The N-terminal and C-terminal domains of ezrin bind membrane proteins and cytoskeleton, respectively (Tsukita et al., 1997). Expression of an ezrin N-terminal domain has been reported to interfere with the endogenous ezrin function as a dominant negative mutant (Algrain et al., 1993; Roumier et al., 2001). To examine if the ezrin influences HIV-1 infection, we prepared human cells expressing the ezrin dominant negative mutant (EZ-N) that is C-terminally tagged with the VSV-G epitope (Algrain et al., 1993). A murine leukemia virus (MLV) vector carrying the EZ-N was inoculated into 293T and TE671 cells expressing CD4 (293T/CD4 and TE671/CD4), and the cells were selected by puromycin. Because the MLV vector genome contained both of the EZ-N and puromycin-resistant genes, it was thought that almost all of the puromycin-resistant cells expressed the EZ-N protein. Western immunoblotting using the anti-VSV-G epitope antibody indicates that the puromycin-resistant cell pools expressed the VSV-G-tagged EZ-N protein as the predicted size (Fig. 1A).

The parental TE671/CD4 and 293T/CD4 cells were susceptible to HIV-1 vector having the X4-tropic NDK HIV-1 Env protein, because the cells endogenously express CXCR4. Transduction titers of the HIV-1 NDK Env vector in TE671/CD4 and 293T/CD4 cells expressing the EZ-N were constantly decreased (Fig. 1B). Such reduction in virus titer was observed when HIV-1 vector having Env protein of a CD4-independent X4-tropic virus strain, mNDK (Dumonceaux et al., 1998), was used as a transduction source (data not shown). In contrast, the EZ-N expression had little effects on the infection of HIV-1 vector having VSV-G protein. Expression of the EZ-N had little effects on cell surface expression of the HIV-1 receptors, CD4 and CXCR4, as monitored by FACS analysis (Fig. 1C). These results suggest that ezrin functions as a positive regulator of HIV-1 infection mediated by the X4-tropic HIV-1 Env but not by the VSV-Env.

To assess whether the EZ-N affects R5-tropic HIV-1 vector transduction, transduction titers of the HIV-1 vector having the R5-tropic JRFL HIV-1 Env protein were measured in target cells transiently transfected with the VSV-G-tagged wild type ezrin (EZ-Wt) or the EZ-N expression plasmid. TE671 cells expressing CD4 and CCR5 (TE671/CD4/R5) were used as the target cells. The EZ-N reduced transduction titer of the X4-tropic NDK HIV-1 vector in the TE671/CD4/R5 cells (Fig. 2A)

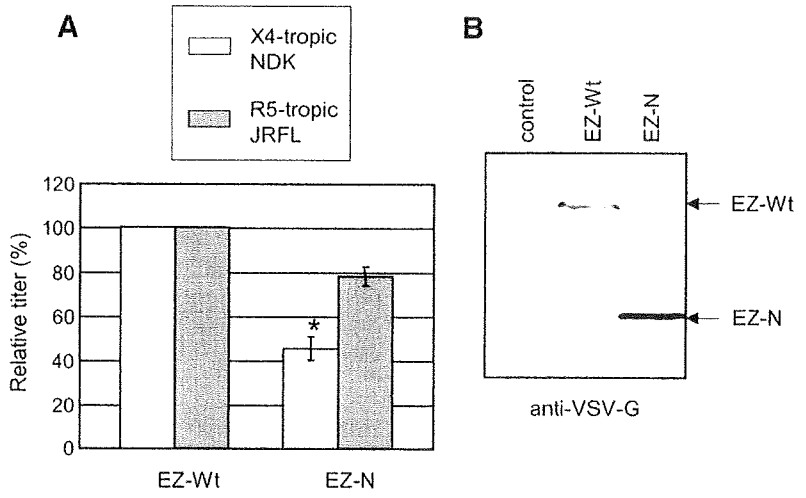

Fig. 2. Effect of ezrin dominant negative mutant on R5-tropic HIV-1 vector transduction. Panel A. Transduction titers of the HIV-1 vector having the X4-tropic NDK (open bar) or R5-tropic JRFL (closed bar) Env protein were measured in TE671/CD4/R5 cells transiently transfected with the wild type ezrin (EZ-Wt) or ezrin dominant negative mutant (EZ-N) expression plasmid. Relative titers to that in the EZ-Wt-transfected cells were indicated. This experiment was repeated three times, and error bars indicate standard deviations. Panel B. Western immunoblotting of the transfected cells was performed using the anti-VSV-G epitope antibody. The EZ-Wt and EZ-N proteins are estimated by their molecular sizes, and are shown by arrows.

compared to the EZ-Wt as control. This result was consistent with that in the TE671/CD4 cells stably expressing the EZ-N (Fig. 1B). However, the EZ-N did not significantly affect the R5-tropic JRFL HIV-1 vector transduction efficiency.

Additionally, we analyzed the effects of the EZ-N on transduction activity and syncytium formation of ecotropic MLV Env proteins in rat XC cells (Kubo et al., 2003). These functions of the ecotropic MLV Env proteins were not affected by the EZ-N

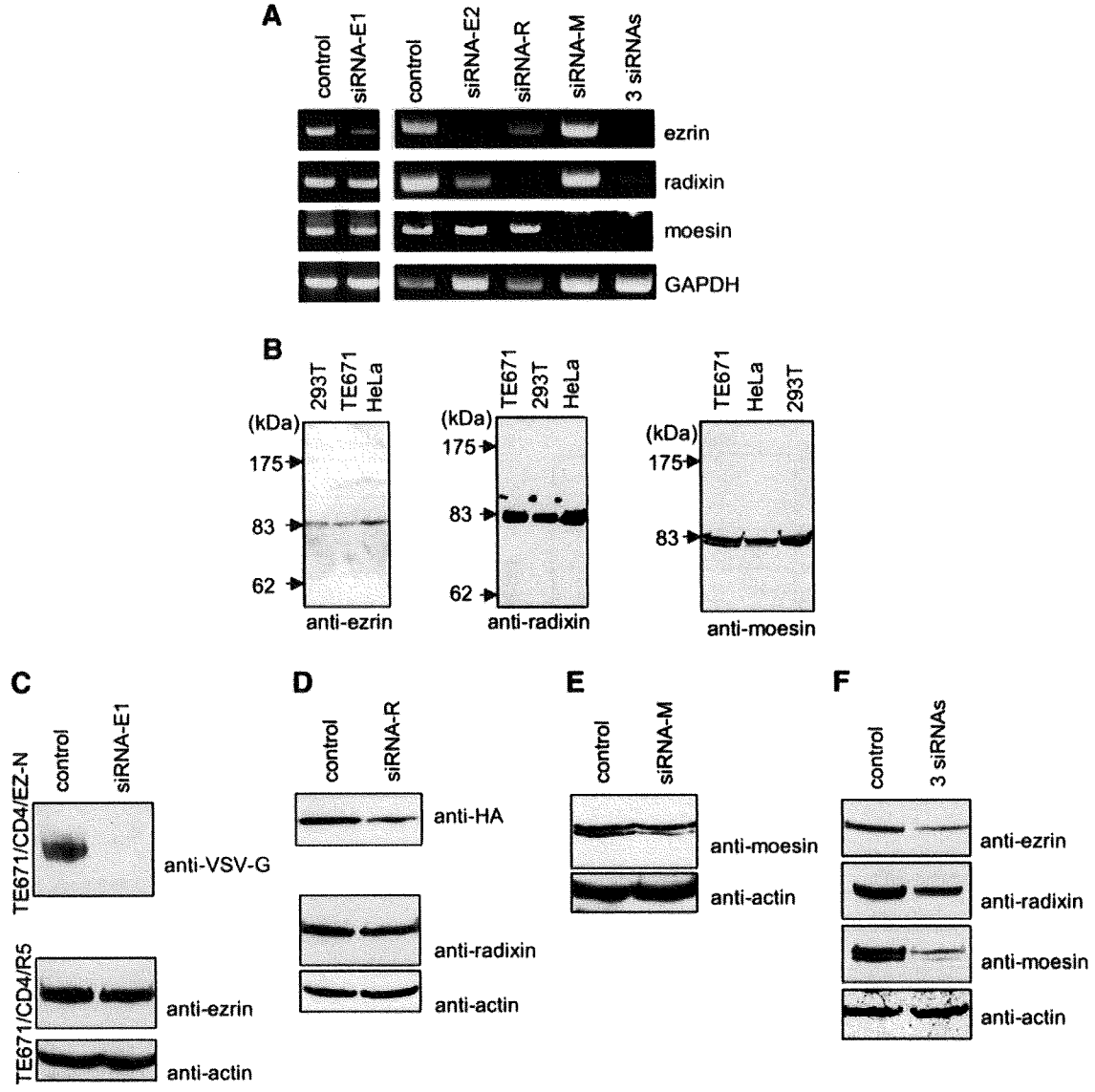

Fig. 3. Knockdown of ERM family proteins by siRNAs. Panel A. Effects of siRNA on ERM mRNA expression. Total RNA samples were isolated from siRNA-GFP-, siRNA-E1-, siRNA-E2-, siRNA-R-, or siRNA-M-transfected TE671/CD4/R5 cells and from cells simultaneously transfected with siRNA-E2, siRNA-R, and siRNA-M (3 siRNAs). Semi-quantitative RT-PCR of these total RNA samples was performed to detect ezrin, radixin, moesin, or GAPDH mRNA. Panel B. ERM family protein expression in human cells. Cell lysates were prepared from 293T, TE671, and HeLa cells, and subjected to Western immunoblotting using the anti-ezrin (left panel), -radixin (middle panel), and -moesin (right panel) antibodies. Molecular size markers are indicated in left side of the panels. Panel C. Effects of siRNA-E1 on ezrin protein expression. Cell lysates were prepared from siRNA-GFP (control)- or siRNA-E1-transfected TE671/CD4 cells expressing the VSV-G-tagged EZ-N mutant. Western immunoblotting of the lysates was performed using the anti-VSV-G epitope antibody. Cell lysates were prepared from siRNA-GFP- or indicated siRNA-E1-transfected TE671/CD4/R5 cells. Western immunoblotting of the lysates was performed using the anti-ezrin or anti-actin antibody. Panel D. Effects of siRNA-R on radixin protein expression. TE671/CD4/R5 cells were transiently transfected with the HA-tagged radixin expression plasmid and an siRNA indicated, and cell lysates were prepared from the transfected cells. Western immunoblotting using the anti-HA antibody was performed. Cell lysates were prepapred from TE671/CD4/R5 cells transfected with the siRNA-GFP or -R. Western immunoblotting using the anti-radixin or anti-actin antibody was performed. Panel E. Effects of siRNA-M on moesin protein expression. Cell lysates were prepared from TE671/CD4/R5 cells transfected with the siRNA-GFP or -M. Western immunoblotting using the anti-moesin or anti-actin antibody was performed. Panel F. Effects of these three siRNAs on ERM protein expression. Cell lysates were prepared from TE671/CD4/R5 cells simultaneously transfected with siRNA-E2, -R, and -R and from cells transfected with siRNA-GFP. Western immunoblotting using anti-ezrin, anti-radixin, anti-moesin, or anti-actin antibody was performed.

expression (data not shown), indicating that ezrin is not associated with the ecotropic MLV Env functions.

Knockdown of ERM family protein expression by siRNA inhibits HIV-1 vector transduction

We were interested in the roles of other ERM family proteins, i.e., radixin and moesin, in HIV-1 infection. siRNAs targeting ezrin, radixin, or moesin mRNA was introduced into the TE671/CD4/R5 cells, and level of the mRNA was monitored by semi-quantitative RT-PCR; siRNA-E1 and -E2 target the ezrin mRNA; siRNA-R targets the radixin mRNA; siRNA-M targets the moesin mRNA. As shown in Fig. 3A, these siRNAs specifically and effectively suppressed expression of corresponding ERM family mRNAs in the TE671/CD4/R5 cells.

We next examined if the siRNAs influence expression levels of the ERM family proteins by Western immunoblotting. As described in manufacture's documents of the antibodies, the commercially available antibodies against the ezrin, radixin, and moesin had strong cross-reactivity due to the high homology within the ERM family proteins. However, we could distinguish moesin from others by the anti-moesin antibody because moesin has smaller molecular size (Fig. 3B, anti-moesin). The moesin was expressed at detectable levels in HeLa and TE671 cells but not in 293T cells. The data with anti-ezrin and anti-radixin antibodies suggest that these proteins were expressed in the three human cells.

To examine siRNA suppression effects on ERM protein expression, we first used anti-VSV-G antibody and examined if exogenous expression of the VSV-G-tagged EZ-N mutant protein in TE671/CD4/EZ-N cells is suppressed by the siRNA against ezrin (siRNA-E1). Target sequence of the siRNA-E1 is located in the N terminal protein-coding region of ezrin mRNA and thus expression of the EZ-N should be suppressed if the siRNA-E1 was functional. Fig. 3C shows that the siRNA-E1 suppressed the expression of the VSV-G-tagged EZ-N mutant protein in TE671/CD4/EZ-N cells, indicating that the siRNA-E1 is functional. As expected, however, we failed to detect the siRNA suppression

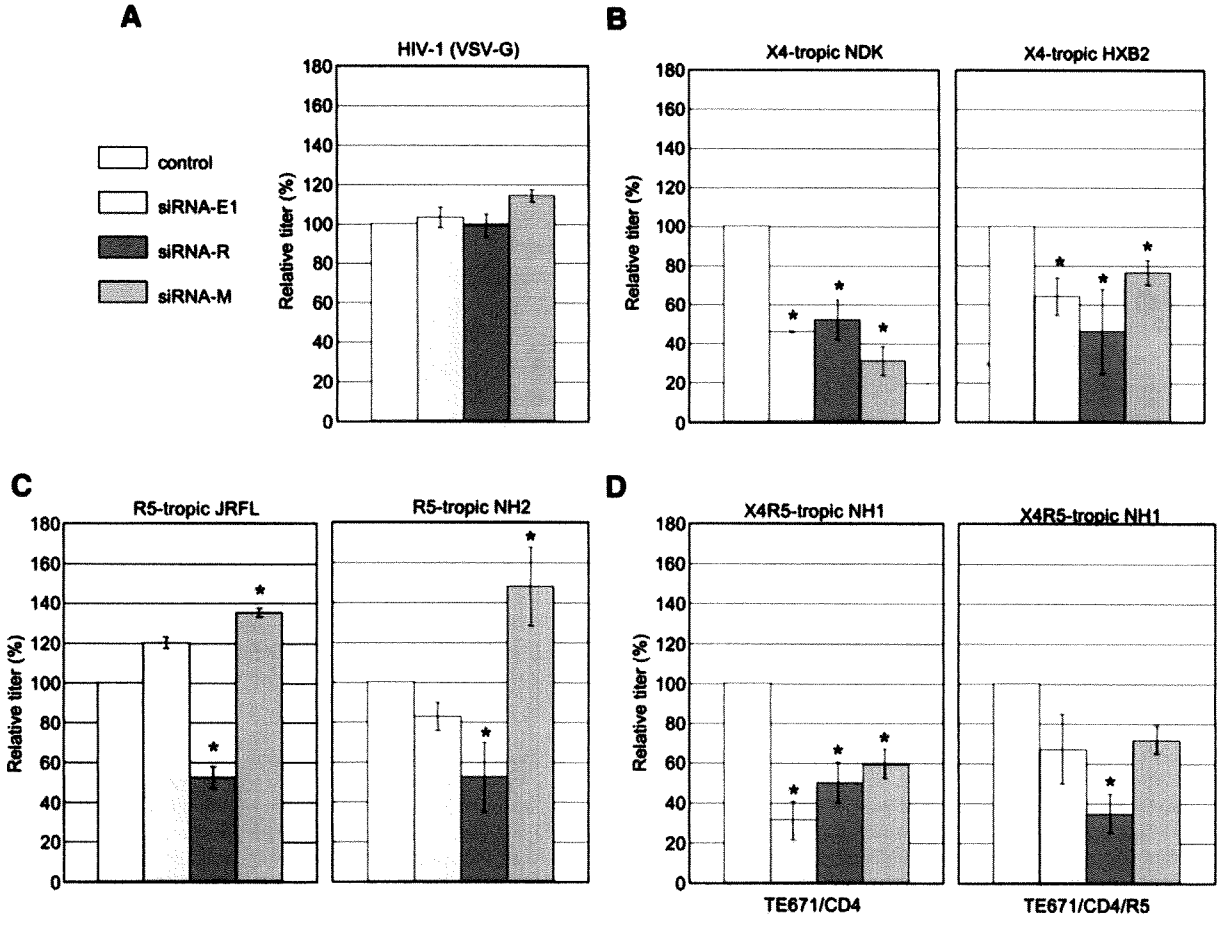

Fig. 4. Effect of siRNAs against ERM family genes on HIV-1 vector transduction. HIV-1 vector pseudotyped with VSV-G (panel A), HIV-1 X4-tropic Env (panel B), or HIV-1 R5-tropic Env (panel C) was inoculated into TE671/CD4/R5 cells transfected with siRNA-GFP, siRNA-E1, siRNA-R, or siRNA-M. HIV-1 vector having the X4R5-tropic NH1 Env protein (panel D) was inoculated into siRNA-transfected TE671/CD4 (left panel) or TE671/CD4/R5 cells (right panel). Relative values to transduction titer in the siRNA-GFP-transfected cells were indicated. This experiment was independently repeated three times. Error bars indicate standard deviations. Asterisks indicate statistical significance (P b 0.05). Panel E. Cell surface expressions of CD4, CXCR4, and CCR5 in the siRNA-transfected TE671/CD4/R5 cells were analyzed by FACS. Closed areas shows cells stained with the FITC-conjugated secondary antibody alone, and open areas do cells stained with the indicated antibodies and the secondary antibody.

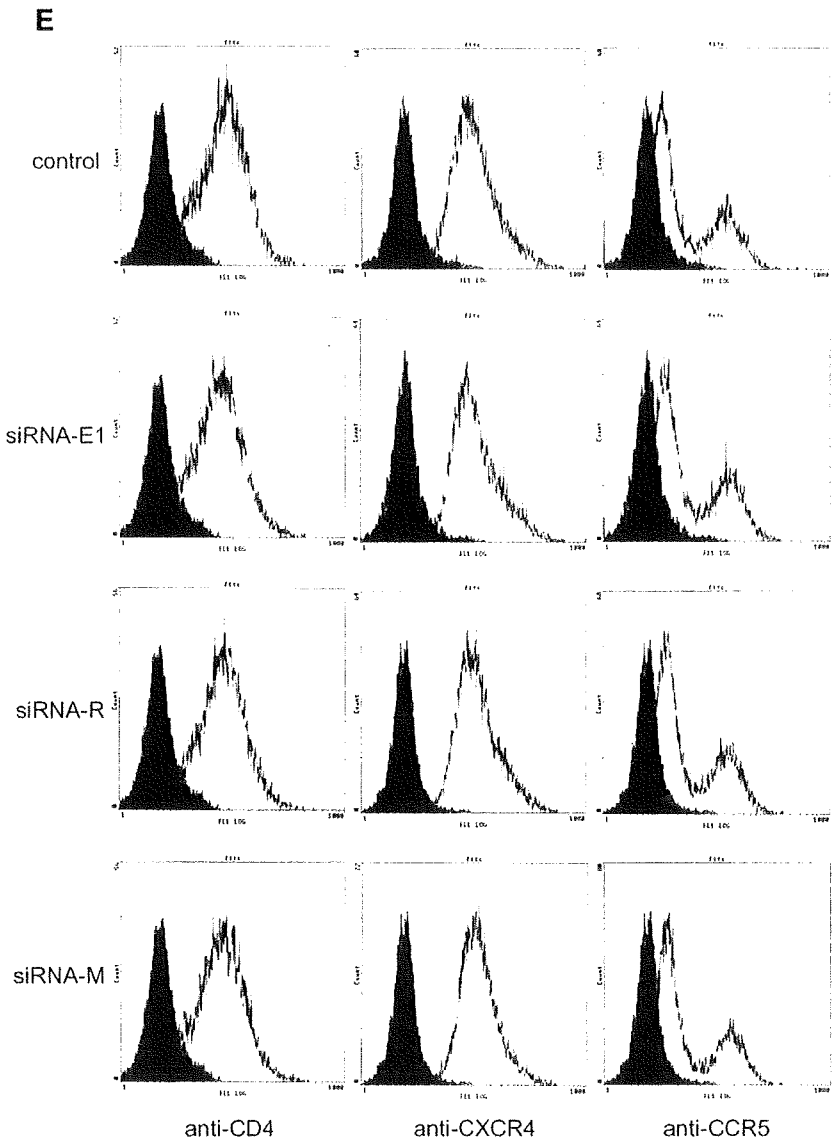

Fig. 4 (continued).

effect in the TE671/CD4/R5 cells with the anti-ezrin antibody (Fig. 3C), because the anti-ezrin antibody recognizes radixin as well. Similarly, we failed to confirm suppression of radixin expression by the siRNA-R with the anti-radixin antibody due to the cross-reactivity of the antibody (Fig. 3D). Therefore, we constructed an expression plasmid of a C-terminally HA-tagged radixin (Rad-HA) to confirm whether the siRNA-R is functional. The Rad-HA level in TE671/CD4/R5 cells co-transfected with the Rad-HA expression plasmid and the siRNA-R was lower than that in cells co-transfected with the Rad-HA expression plasmid and the siRNA against GFP (Fig. 3D). In contrast, we could confirm the siRNA-M-mediated suppression of endogenous moesin protein expression with anti-moesin antibody, because molecular size of moesin is smaller than ezrin and radixin (Fig. 3E). When TE671/CD4/R5 cells were simultaneously transfected with the siRNA-E2, -R, and -M, suppressed expression of ezrin, radixin, and moesin proteins was detected using the each antibodies (Fig. 3F). Taken together, our results suggest that these siRNAs inhibit the corresponding protein expression via suppression of mRNA expression.

Transduction titer of the VSV-G vector was not affected by these siRNAs (Fig. 4A), suggesting that VSV-envelope-mediated infection proceeds via ERM-protein independent pathway as already reported (Kameoka et al., 2007). In contrast, transduction titers of the X4-tropic NDK and HXB2 vectors were decreased uniformly by the introduction of siRNA against ezrin, radixin, or moesin (Fig. 4B). X4-tropic transduction efficiency of the X4R5-tropic NH1 vector was also inhibited in TE671/CD4 cells (Fig. 4D), because CC5R is not expressed in the cells. These results were consistent with the data on the ezrin dominant negative mutant (Figs. 1 and 2).

The siRNA-R decreased the titers of the R5-tropic vector and the siRNA-M rather increased the titers (Fig. 4C). These changes were highly reproducible in the repeated experiments.

These effect of the siRNA-mediated knock down of the ERM proteins on the HIV-1 infection was not induced by altered cell surface expression of the HIV-1 receptors, because cell surface expression of the HIV-1 receptors, CD4, CXCR4, and CCR5, were not changed by the siRNAs (Fig. 4E). These results suggest that all of the three ERM family proteins function as positive regulators of the X4-tropic HIV-1 infection, whereas radixin and moesin function positive and negative regulators, respectively, of the R5-tropic HIV-1 infection.

Transduction efficiency of the dual-tropic NH1 vector in TE671/CD4 cells was suppressed by each of the siRNA (Fig. 4D) as that of the X4-tropic vector. Because TE671/CD4 cells do not express CCR5, entry of the dual-tropic NH1 vector occurs only through CXCR4 in the cells. The moesin knockdown in TE671/CD4/R5 cells did not enhance transduction efficiency of the dual-tropic NH1 vector, but did that of the R5-tropic vector. Entry of the NH1 vector was thought to occur through both of CXCR4 and CCR5 in TE671/CD4/R5 cells. Therefore, the effect of moesin knockdown on the dual-tropic vector in TE671/CD4/R5 cells should be different from that on the R5-tropic vector.

To examine if expression of siRNA-resistant ezrin mRNA abrogate the inhibitory effect of ezrin siRNA on the X4-tropic HIV-1 vector transduction, we examined effects of siRNA-E2, which targets 3 untranslated region (3 UTR) of the ezrin mRNA, on the X4-tropic virus transduction in the TE671/CD4 cells. The siRNA-E2 reduced the endogenous ezrin mRNA level (Fig. 3A), but did not suppress exogenous expression of VSV-G-tagged wild type ezrin (Fig. 5A), because the exogenous mRNA encoding the VSV-G-tagged ezrin does not contain the 3 UTR. The siRNA-E2 transfection into TE671/CD4 cells decreased transduction titer of the NDK HIV-1 vector (Fig. 5B) as the siRNA-E1 did (Fig. 4B). Expression of the siRNA-resistant ezrin, i.e., VSV-G-tagged ezrin wild type protein, abrogated the inhibitory effect of the siRNA-E2 (Fig. 5B). The VSV-G-tagged ezrin expression alone did not affect the HIV-1 vector transduction efficiency. These results support the argument that ezrin is important for increasing efficiency of the X4-tropic HIV-1 infection.

Effects of ERM-family-targeting siRNAs on cell–cell fusion mediated by HIV-1 Env proteins

To assess whether the ERM family proteins play roles in HIV-1-Env-mediated membrane fusion, we examined if the ezrin dominant negative mutant (EZ-N) and siRNAs against the ERM family proteins influence cell–cell fusion in co-culture of target cells and NDK Env-expressing 293T cells. In this co-culture system, we can monitor cell–cell fusion via interaction of HIV-1 Env and HIV-1 infection receptors by using the -galactosidase activity (see Materials and methods). NDK Env-mediated cell–cell fusion was inhibited by introduction of either the EZ-N protein (Fig. 6A), siRNA-E2, -R, or -M (Fig. 6B) into the receptor expressing cells, consistent with the results obtained from HIV-1 vector transduction assay (Figs. 1B and 4B). Similarly, JRFL-Env-mediated cell–cell fusion was inhibited by ezrin and radixin siRNAs (Fig. 6C), although the ezrin siRNA had no effect on the R5-tropic HIV-1 vector transduction efficiency (Fig. 4C). The siRNA-M enhanced the vector transduction of the R5-tropic vector, whereas such enhancement was not observed in the cell fusion. These effects were highly reproducible in the repeated experiments.

Discussion

In this study, we examined potential roles of the ERM proteins in HIV-1 entry. A recent study described the similar topic, in

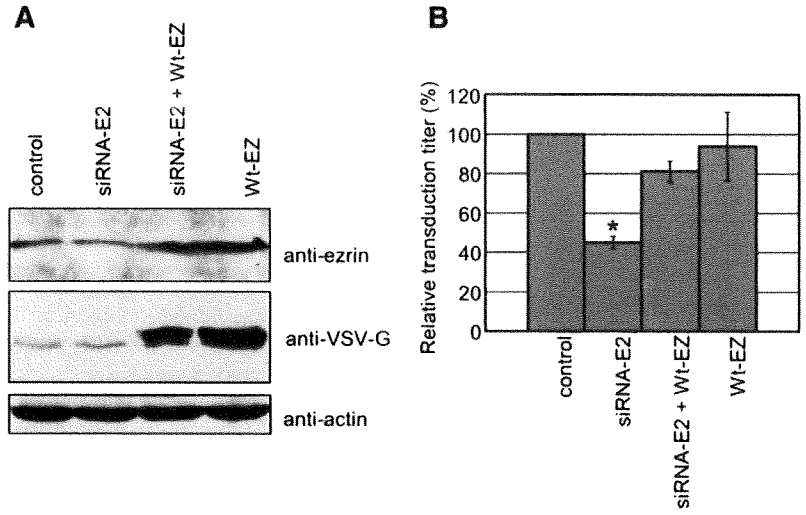

Fig. 5. Abrogation of inhibitory effect of ezrin knockdown on HIV-1 vector transduction by exogenous ezrin expression. Panel A. Cell lystaes were prepared from TE671/CD4/R5 cells transfected with the siRNA-GFP alone, from cells transfected with siRNA-E2 alone, from cells co-transfected with the VSV-G-tagged wild type ezrin expression plasmid and the siRNA-E2, and from cells transfected with the ezrin expression plasmid alone. Westerm immunoblotting of the cell lystaes was performed using the anti-ezrin (upper panel), anti-VSV-G epitope (middle panel), or anti-actin (lower panel) antibody. Panel B. The transfected cells were inoculated with the HIV-1 vector having the NDK Env protein. Relative values to transduction titer in the siRNA-GFP-transfected cells were indicated. This experiment was independently repeated three times. Error bars show standard deviations. Asterisks indicate statistical significance (P b 0.05).

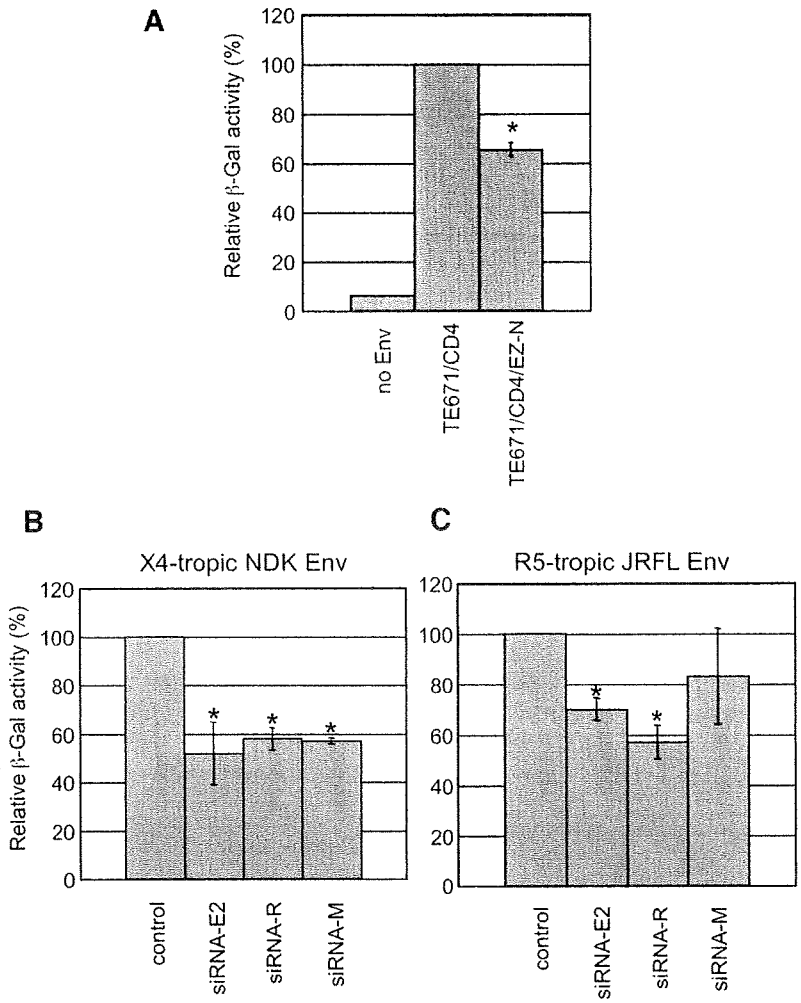

Fig. 6. Effect of ezrin dominant negative mutant and siRNAs against ERM family proteins on HIV-1-Env-mediated cell–cell fusion. 293T cells were transfected with the NDK (panels A and B) or JRFL (panel C) Env expression plasmid. TE671/CD4 or TE671/CD4/EZ-N cells transfected with the LTR-LacZ construct were added onto 293T cells transfected with the NDK Env expression plasmid (panel A). TE671/CD4/R5 cells were co-transfected with the each siRNA as indicated and the LTR-LacZ plasmid. The transfected TE671/CD4/R5 cells were added onto the transfected 293T cells. -Galactosidase activities of their cell lystaes were measured as described in Materials and methods. Relative values to -galactosidase activity of the mixed culture of the siRNA-GFP-transfected TE671/CD4/R5 cells and the Env-transfected 293T cells were indicated. This experiment was repeated three times, and error bars indicate standard deviations. Asterisks indicate statistical significance (P b 0.05).

which the authors showed that the moesin regulates stable microtubule formation and inhibits transduction of HIV-1 vectors having VSV-G protein in the rat cells (Naghavi et al., 2007). Our study deals with the similar topic but rather focused on the roles of the three ERM proteins in HIV-1-Env-mediated infections of human cells rather than VSV-Env-mediated infection of the rodent cells. Our study thus could reveal a hitherto unappreciated regulation mechanism, a pleiotropic regulation of HIV-1 infection by the ERM proteins.

Each of the siRNA against the ERM family proteins as well as the dominant negative mutant of ezrin inhibited transduction of X4-tropic HIV-1 vectors (Figs. 1B and 4B). These inhibitions were unlikely to be due to the reduced binding events of HIV-1 Env to the infection receptors, because the levels of cell surface expression of the CD4 and CXCR4 were similar in the ERM-suppression-positive and -negative cells (Figs. 1C and 4E). Similarly, the inhibitions were unlikely to be due to the overall reductions in the HIV-1 replication processes, because VSV-G-mediated HIV-1 transductions were not affected by the ERM suppression (Figs. 1B and 4A). Alternatively, our results strongly suggest that the ERM suppression induced specific inhibition of the X4-tropic HIV-1 infection at the entry step(s). Correlation between the X4-tropic vector transduction inhibition and cell–cell fusion inhibition (Figs. 4B and 6B) suggests that a key site of action for the siRNA-mediated inhibition is the membrane fusion. This in turn implies that the ERM proteins individually play positive roles in the membrane fusion mediated by interactions of X4-tropic Env and infection receptors.

Interestingly, transductions of the R5-tropic HIV-1 vectors were inhibited by the radixin siRNA alone, but were not by the ezrin and moesin siRNAs (Fig. 4C). The moesin siRNA rather increased the R5-tropic HIV-1 vector transductions. These results suggest that radixin of the ERM family is a key molecule for the efficient R5-tropic HIV-1 infection, whereas moesin rather